THE DYNAMICS AND CONTROL OF LARGE FLEXIBLE SPACE STRUCTURES - XI

FINAL REPORT

NASA GRANT: NSG-1414, Supplement 10

by

Peter M. Bainum
Professor of Aerospace Engineering
Principal Investigator

and

A.S.S.R. Reddy
Assistant Professor
Co-Investigator

and

Cheick M. Diarra
Feiyue Li
Graduate Research Assistants

August 1988

DEPARTMENT OF MECHANICAL ENGINEERING
SCHOOL OF ENGINEERING
HOWARD UNIVERSITY
WASHINGTON, D.C. 20059

ABSTRACT

A mathematical model is developed to predict the dynamics of the proposed Spacecraft Control Laboratory Experiment during the station keeping phase. The Shuttle and reflector are assumed to be rigid, while the mast connecting the Shuttle to the reflector is assumed to be flexible with elastic deformations small as compared with its length. It is seen that in the presence of gravity-gradient torques, the system assumes a new equilibrium position primarily due to the offset in the mast attachment point to the refector from the reflector's mass center. Control is assumed to be provided through the Shuttle's three torquers and through six actuators located by pairs at two points on the mast and at the reflector mass center. Numerical results confirm the robustness of an LQR derived control strategy during station keeping with maximum control efforts significantly below saturation levels. The linear regulator theory is also used to derive control laws for the linearized model of the rigidized SCOLE configuration where the mast flexibility is not included. It is seen that this same type of control strategy can be applied for the rapid single axis slewing of the SCOLE through amplitudes as large as 20 deg. These results provide a definite trade-off between the slightly larger slewing times with the considerable reduction in over-all control effort as compared with the results of the two point boundary value problem (TPBVP) application of Pontryagin's Maximum Principle. In connection with the TPBVP, a useful numerical solution procedure for minimum time, 2-D and 3-D attitude maneuvers of a rigid spacecraft is developed and applied to the SCOLE system. Both singular and nonsingluar cases can be handled. The minimum time is determined by sequentially shortening the slewing time. It is shown that one of the

four initial costates associated with the quaternions can be arbitrarily selected without affecting the optimal controls, thus resulting in a simplification of the computation. Finally, a stability criterion for a controller which operates in the continuous time domain but depends on discretized input data is developed and relates the maximum tolerable discretization step size to the damping ratio and undamped frequency of any mode in the system model. Computational requirements for the estimator and controller are evaluated based on a type 80387 microprocessor, and assuming that the number of actuators and sensors are a certain fraction of the number of state components.

TABLE OF CONTENTS

LIST OF FIGURES

INTRODUCTION

The present grant, NSG-1414, Supplement 10, represents an extension to the research effort initiated and accomplished in previous grant years (May 1977 - March 1987) and reported in Refs. 1-14*. The attitude and shape control of very large inherently flexible proposed future spacecraft systems is being investigated. Possible future applications of such large spacecraft systems (LSS) include: large scale multi-beam antenna communication systems; Earth observation and resource sensing systems; orbitally based electronic mail transmission; as platforms for orbital based telescope systems; and as in-orbit test models designed to compare the performance of flexible LSS systems with that predicted based on computer simulations and/or scale model Earth-based laboratory experiments. In recent years the grant research has focused on the orbital model of the Spacecraft Control Laboratory Experiment (SCOLE) first proposed by Taylor and Balakrishnan[15] in 1983.

The present report is divided into six chapters. Chapter II is based on a paper presented at the 1988 AIAA/AAS Astrodynamics Conference which describes the development of a mathematical model to predict the dynamics and control of the SCOLE configuration in-orbit during station keeping. The flexibility of the mast which connects the reflector to the Shuttle is included in the model. In accordance with the SCOLE design challenge[15] the attachment point between the mast and the reflector is considered to be offset in two cartesian directions from the mass center of the reflector. The linear regulator theory is used to derive both orientation and mast vibration suppression control laws.

---

* References cited in this report are listed separately at the end of each chapter.

In the following chapter (Chapter III) the same linear regulator theory techniques are applied to develop control laws of a rigid model of the SCOLE which could be used for rapid single-axis slewing through as much as 20 deg. These control laws could provide an attractive alternative to the slewing strategies[14] based on the two point boundary value problem associated with Pontryagin's Maximum Principle where a trade-off could be made between the noticeable savings in control effort and the increased slewing times associated with the LQR applications. Chapter III is based on a paper accepted for presentation at the 39th International Astronautical Congress in October 1988.

Chapter IV represents a completely revised version of a paper presented at the AIAA 26th Aerospace Sciences Meeting and describes a numerical approach for solving general three dimensional rigid spacecraft minimum time attitude maneuvers. In place of the total slewing time an integral of a quadratic function of the controls is used as the cost function and allows for the treatment of both the singular and nonsingular problems in a unified way. The resulting two point boundary value problem is developed by applying the Maximum Principle to the system and solved by using a quasilinearization algorithm.

In the following chapter (Chapter V) aspects of the computational requirements for the implementation of the controller are discussed. An improved stability criterion for a controller, designed to function in the continuous time domain, but which receives discretized observational inputs, is developed. An expression for the maximum tolerable discretization step size is derived in terms of the undamped frequency and damping ratio of any mode in the continuous-time system model. In the second part of Chapter V

the (on-board) computational requirements for the estimator and controller are evaluated based on a type 80387 microprocessor, and assuming that the number of actuators and sensors are a certain fraction of the number of state components.

Finally, Chapter VI describes the main general conclusions together with future recommendations. The effort described here is being continued during the 1988-89 grant year in accordance with our most recent proposal.[16]

References - Chapter I

1. Bainum, P.M. and Sellappan, R., "The Dynamics and Control of Large Flexible Space Structures," Final Report NASA Grant: NSG-1414, Part A: Discrete Model and Modal Control, Howard University, May 1978.

2. Bainum, Peter M., Kumar, V.K., and James, Paul K., "The Dynamics and Control of Large Flexible Space Structures," Final Report, NASA Grant: NSG-1414, Part B: Development of Continuum Model and Computer Simulation, Howard University, May 1978.

3. Bainum, P.M. and Reddy, A.S.S.R., "The Dynamics and Control of Large Flexible Space Structures II," Final Report, NASA Grant NSG-1414, Suppl. I, Part A: Shape and Orientation Control Using Point Actuators, Howard University, June 1979.

4. Bainum, P.M., James, P.K., Krishna, R., and Kumar, V.K., "The Dynamics and Control of Large Flexible Space Structures II," Final Report, NASA Grant NSG-1414, Suppl. 1, Part B: Model Development and Computer Simulation, Howard University, June 1979.

5. Bainum, P.M., Krishna, R., and James, P.K., "The Dynamics and Control of Large Flexible Space Structures III," Final Report, NASA Grant NSG-1414, Suppl. 2, Part A: Shape and Orientation Control of a Platform in Orbit Using Point Actuators, Howard University, June 1980.

6. Bainum, P.M. and Kumar, V.K., "The Dynamics and Control of Large Flexible Space Structures III," Final Report, NASA Grant NSG-1414, Suppl. 2, Part B: The Modelling, Dynamics and Stability of Large Earth Pointing Orbiting Structures, Howard University, September 1980.

7. Bainum, P.M., Kumar, V.K., Krishna, R. and Reddy, A.S.S.R., "The Dynamics and Control of Large Flexible Space Structures IV," Final Report, NASA Grant NSG-1414, Suppl. 3, NASA CR-165815, Howard University, August 1981.

8. Bainum, P.M., Reddy, A.S.S.R., Krishna, R., Diarra, C.M., and Kumar, V.K., "The Dynamics and Control of Large Flexible Space Structures V", Final Report, NASA Grant NSG-1414, Suppl. 4, NASA CR-169360, Howard University, August 1982.

9. Bainum, P.M., Reddy, A.S.S.R., Krishna, R., and Diarra, C.M., "The Dynamics and Control of Large Flexible Space Structures VI," Final Report NASA Grant NSG-1414, Suppl. 5, Howard University, Sept. 1983.

10. Bainum, P.M., Reddy, A.S.S.R., Krishna, R., Diarra, C.M. and Ananthakrishnan, S., "The Dynamics and Control of Large Flexible Space Structures-VII," Final Report NASA Grant NSG-1414, Suppl. 6, Howard University, June 1984.

11. Bainum, P.M., Reddy, A.S.S.R., Diarra, C.M. and Ananthakrishnan, S., "The Dynamics and Control of Large Flexible Space Structures-VIII," Final Report NASA Grant NSG-1414, Suppl. 7, Howard University, June 1985.

12. Bainum, P.M., Reddy, A.S.S.R., and Diarra, C.M., "The Dynamics and Control of Large Flexible Space Structures-IX," Final Report NASA Grant NSG-1414, Suppl. 8, Howard University, July 1986.

13. Bainum, P.M., Reddy, A.S.S.R., Li, Feiyue, and Diarra, C.M., "The Dynamics and Control of Large Flexible Space Structures X-Part I", Final Report NASA Grant NSG-1414, Suppl. 9, Howard University, August 1987.

14. Bainum, P.M., Reddy, A.S.S.R., Diarra, C.M., and Li, Feiyue, "The Dynamics and Control of Large Flexible Space Structures X-Part II", Final Report NASA Grant NSG-1414, Suppl. 9, Howard University, January 1988.

15. Taylor, L.W. and Balakrishnan, A.V., "A Mathematical Problem and a Spacecraft Control Laboratory Experiment (SCOLE) Used to Evaluate Control Laws for Flexible Spacecraft...NASA/IEEE Design Challenge," (Rev.), January 1984. (Originally presented at AIAA/VP&SU Symposium on Dynamics and Control of Large Structures, June 6-8, 1983.)

16. Bainum, P.M. and Reddy, A.S.S.R., "Proposal for Research Grant on: "The Dynamics and Control of Large Flexible Space Structures XII", Howard University (submitted to NASA), October 15, 1987.

II. THE DYNAMICS AND CONTROL OF THE ORBITING SPACECRAFT CONTROL LABORATORY EXPERIMENT (SCOLE) DURING STATION KEEPING

Abstract

A mathematical model is developed to predict the dynamics of the proposed orbiting Spacecraft Control Laboratory Experiment during the station keeping phase. The Shuttle as well as the reflector are assumed to be rigid, the mast is flexible and is assumed to undergo elastic displacements very small as compared with its length. The equations of motion are derived using a Newton-Euler formulation. The model includes the effects of gravity, flexibility, and orbital dynamics. The control is assumed to be provided to the system through the Shuttle's three torquers, and through six actuators located by pairs at two points on the mast and at the mass center of the reflector. At each of the locations, an actuator acts parallel to the roll axis while the other one acts parallel to the pitch axis. It is seen that, in the presence of gravity-gradient torques in the system dynamics, the system assumes a new equilibrium position about which the equations must be linearized, primarily due to the offset in the mast attachment point to the reflector. The linear regulator theory is used to derive control laws for the linear model of the SCOLE including the first four flexible modes. Numerical results confirm the robustness of this control strategy for station keeping with maximum control efforts significantly below saturation levels.

I. Introduction

The problem of maneuvering a flexible spacecraft while suppressing the induced vibrations is becoming increasingly important. NASA is involved in studies which are concerned with the control of flexible bodies carried by a Shuttle in an Earth orbit. Similar experiments are being conducted in Earth-based laboratories. It is then desirable to derive a formulation which can accommodate both types of experiments.

NASA is currently involved in at least two experimental programs to test techniques derived for active control of flexible space structures.

In several versions of a recent paper, SCOLE[1] (Spacecraft Control Laboratory Experiment), Lawrence W. Taylor, Jr. and A.V. Balakrishnan have described the first which is ground based. It is a laboratory experiment based on a model of the Shuttle connected to a flexible beam with a reflecting grillage mounted at the end of the beam (Fig. 1). As a part of the design challenge, the authors stressed the need to directly compare competing control design techniques and discussed the feasibility of such a direct comparison. Concern would be given to modeling order reduction, fault management, stability, and dynamic systems. The second experimental program is known as Control of Flexible Spacecraft (COFS)[2] and consists of experiments designed to control flexible bodies carried by a Shuttle in an Earth orbit. Because of the cost and risks involved in testing control techniques in space, COFS includes laboratory simulations of similar experiments which will precede the space test. Therefore, in assuring the success of both SCOLE and COFS, mathematical modeling and computer simulation are required.

To accurately model and simulate flexible spacecraft, one needs a thorough knowledge of its structural behavior. In a paper[3], subsequent to the design challenge, the modal shapes and frequencies for the SCOLE system were derived. In reference 3, the SCOLE system is assumed to be described by partial differential equations in which the variables separate.

Undertaken in this study is the modeling of the three dimensional dynamics of the SCOLE configuration based on the Eulerian technique. This consists in isolating an elemental mass of the system in its deformed state and deriving its angular momentum taken at the mass center of the Orbiter. The position vector extending from the origin of the coordinate system to the elemental mass of the mast or the reflector accounts for the elastic displacements. The expressions for these displacements are derived from the mode shape functions generated during the three dimensional structural analysis of the system.

The equations obtained for the elemental mass of the components of the system are integrated over the mass of the entire system to yield its angular momentum about the mass center of the Orbiter. The derivative of the system angular momentum with respect to time is equated to the gravity-gradient (and other external) torques on the system about the same point. Such a vectorial equation, when projected along the three axes of rotation, yields the system rotational equations of motion. These rotational equations of motion are then linearized to yield a model which provides the basis for the control law synthesis developed in this study.

II. Angular Momentum of the SCOLE System

A. Angular Momentum of the Shuttle about its Mass Center, G

The angular momentum of the Shuttle, taken as a rigid body, about its center of mass, G is

$$\vec{H}_{S/G} = \bar{\bar{I}}_{S/G}\,\vec{\Omega}_{S/R_0} \qquad (1)$$

where $\bar{\bar{I}}_{S/G}$ is the inertia tensor of the Shuttle and $\vec{\Omega}_{S/R_0}$ the Shuttle's inertial angular velocity.

B. Angular Momentum of the Beam About G

Consider an element of mass, dm, of the beam located at some point, P, such that (Fig. 1)

$$\vec{GP} = \bar{r}_0 + \bar{q} \qquad (2)$$

where $\bar{r}_0 = -z\hat{k}$ is the position vector of P in the underformed state; $\bar{q}\,(z,t) = u(z,t)\,\hat{i} + v(z,t)\hat{j}$ in which, u and v are the x and y components of the mode shape vector, respectively.

The angular momentum of dm about G, $d\vec{H}_{M/G}$ is given by:

$$d\vec{H}_{M/G} = \bar{r} \times \frac{d}{dt}\,(\bar{r})\,|_{R_0}\,dm \qquad (3)$$

where

$$\bar{r} = -z\hat{k} + u\hat{i} + v\hat{j}$$

Equation (3) may be expanded, after substitution, to yield:

$$d\vec{H}_{M/G} = \{[z(\dot{v} + \Omega_z u) + v(\Omega_x v - \Omega_y u) - z^2\,\Omega_x]\hat{i}$$

$$+ [-z(\dot{u} - \Omega_z v) + u(\Omega_y u - \Omega_x v) + z^2\Omega_y]\hat{j}$$

$$+ [\dot{u}(v + \Omega_z u) - v(\dot{u} - \Omega_z v) + z(u\Omega_x + v\Omega_y)]\hat{k}\}\,dm \qquad (4)$$

where

$$u(z,t) = \sum_n p^n(t)\,S_x^n(z) \text{ and } v(z,t) = \sum_n p^n(t)\,S_y^n(z)$$

The total angular momentum of the mast about G is obtained by integrating Equation (4) over the total length of the mast.

$$\vec{H}_{M/G} = \int_0^{-L} d\vec{H}_{m/G} \qquad (5)$$

To simplify the notations, let

$$f_i(\beta) = \{A_i(L\,\frac{\cos\beta L}{\beta} - \frac{\sin\beta L}{\beta^2})$$

$$+ B_i\,(L\,\frac{\sin\beta L}{\beta} + \frac{\cos\beta L}{\beta^2} - \frac{1}{\beta^2})$$

$$+ C_i\,(\frac{\sinh\beta L}{\beta^2} - L\,\frac{\cosh\beta L}{\beta})$$

$$+ D_i\,(L\,\frac{\sinh\beta L}{\beta} - \frac{\cosh\beta L}{\beta^2} + \frac{1}{\beta^2})\}$$

After substitution of f_i and $\frac{M}{L}$ for ρ, where M = mass of the mast, in the expression of $\vec{H}_{M/G}$ and considering only the effect of a single mode (for demonstration purposes here, with frequency ω) one arrives at:

$$\vec{H}_{M/G} = \frac{M}{L}\{[\Omega_z \cos(\omega t+\alpha)f_1 - \omega \sin(\omega t+\gamma)f_2 - \Omega_x L^3/3]\,\hat{i}$$

$$+ [\omega \sin(\omega t+\alpha)f_1 - \Omega_z \cos(\omega t+\gamma)f_2 - \Omega_y L^3]\,\hat{j}$$

$$+ [\Omega_x \cos(\omega t+\alpha)f_1 + \Omega_y \cos(\omega t+\gamma)f_2]\,\hat{k}\} \qquad (6)$$

C. Angular Momentum of the Reflector About, G

Since small deflections are assumed for the beam, the reflector can be assumed to be located at a constant distance from G, the Shuttle mass center.

Using the transfer theorem for the angular momentum[4], the angular momentum, $\vec{H}_{R/G}$, of the reflector, assumed rigid, about G can be expressed as:

$$\vec{H}_{R/G} = \bar{\bar{I}}_{R/G_1}\,\vec{\Omega}_{R/R_0} + M_R\,\vec{GG}_1 \times \frac{d}{dt}\,(\vec{GG}_1)|_{R_0} \qquad (7)$$

where $\bar{\bar{I}}_{R/G_1}$ = the inertia tensor of the reflector expressed at G_1, its center of mass, and $\vec{\Omega}_{R/R_0} = \vec{\Omega}_{R/S} + \vec{\Omega}_{S/R_0}$ (respectively, the reflector's inertial angular velocity, its angular velocity relative to the Shuttle, and the Orbiter's inertial angular velocity) are both expressed in the same coordinate system, R_2, moving with the reflector.

D. Angular Momentum of the System About G

The angular momentum of the system about G, $\vec{H}_{syst/G}$, is given by the sum of the angular momentum of each of the three components evaluated about the same point, G.

$$\vec{H}_{syst/G} = \vec{H}_{S/G} + \vec{H}_{M/G} + \vec{H}_{R/G} \qquad (8)$$

III. Rotational Equations of Motion (Torque Free)

The rotational equations of motion for the system, when free of all external torques, are obtained as:

$$(\dot{\vec{H}}_{syst/G})|_{R_0} = \dot{\vec{H}}_{syst/G/S} + \vec{\Omega}_{S/R_0} \times \vec{H}_{syst/G} = \vec{0} \qquad (9)$$

The vector equation (9) itself is equivalent to

$$\dot{H}_x + \Omega_y H_z - \Omega_z H_y = 0 \quad \text{(roll)}$$

$$\dot{H}_y + \Omega_z H_x - \Omega_x H_z = 0 \quad \text{(pitch)}$$

$$\dot{H}_z + \Omega_x H_y - \Omega_y H_x = 0 \quad \text{(yaw)} \qquad (10)$$

When the gravity-gradient torques taken at the Shuttle center of mass are included in the equations of motion, the linear system dynamics appear in the following state form[5]:

$$\dot{X} = AX + C \qquad (11)$$

where C is a constant and $X = (\psi,\theta,\phi,\dot{\psi},\dot{\theta},\dot{\phi})^T$, involving the Euler roll, pitch, and yaw angles (and their rates), respectively.

This indicates that the system equilibrium position is no longer: $\psi_0 = \theta_0 = \phi_0 = 0$, due to the offset (X,Y) in the attachment point of the beam to the reflector (Fig. 1).

Let ψ_e, θ_e, and ϕ_e be the equilibrium position for this configuration of the system. Then,

$$\psi = \psi_e + \eta_1 \quad \text{and} \quad \dot{\psi} = \dot{\eta}$$

$$\theta = \theta_e + \eta_2 \; ; \quad \dot{\theta} = \dot{\eta}_2$$

$$\phi = \phi_e + \eta_3 \; ; \quad \dot{\phi} = \dot{\eta}_3$$

The new state vector is $[\eta_1, \eta_2, \eta_3, \dot{\eta}_1, \dot{\eta}_2, \dot{\eta}_3]^T$.

Also ψ_e, θ_e, and ϕ_e satisfy

$$a_1 \psi_e + a_2 \theta_e + a_3 \phi_e = -a_{19}$$

$$a_7 \psi_e + a_8 \theta_e + a_9 \phi_e = -a_{20}$$

$$a_{13} \psi_e + a_{14} \theta_e + a_{15} \phi_e = -a_{21}$$

this simulataneous system is solved using

$$[a] = [A] [\psi_e, \theta_e, \phi_e]^T \Rightarrow [\psi_e, \theta_e, \phi_e]^T = [A^{-1}] [a]$$

After substituting the new state vector in the equations describing the system dynamics, linearizing them about the new equilibrium position, recasting them into state format, one arrives at a system which can be cast in the form: $\dot{\bar{\eta}} = A' \bar{\eta}$ (where $a'_1 \rightarrow a'_{18}$ are constants)[5]

$$A' = \begin{bmatrix} 0 & 0 & 0 & 1 & 0 & 0 \\ 0 & 0 & 0 & 0 & 1 & 0 \\ 0 & 0 & 0 & 0 & 0 & 1 \\ a'_1 & a'_2 & a'_3 & a'_4 & a'_5 & a'_6 \\ a'_7 & a'_8 & a'_9 & a'_{10} & a'_{11} & a'_{12} \\ a'_{13} & a'_{14} & a'_{15} & a'_{16} & a'_{17} & a'_{18} \end{bmatrix}$$

The open-loop system in this configuration is unstable due to the unfavorable inertia distribution.

IV. Generic Mode Equations [5,6]

The generic mode equations are obtained by taking the modal components of all internal, external and inertial forces acting on the system, i.e.,

$$\int_M \bar{\phi}_n \cdot [\bar{a}_{cm} + \ddot{\bar{r}} + 2\bar{\omega}\dot{\bar{x}}\bar{r} + \dot{\bar{\omega}}\bar{x}\bar{r} + \bar{\omega}x(\bar{\omega}x\bar{r})] \, dm = \int_M \bar{\phi}_n \cdot [L(\bar{q})/_{dm} + \bar{f} + \bar{e}] \, dm \qquad (12)$$

where $\bar{\phi}_n$ is the n^{th} mode shape vector; $\bar{L}$ is a linear operator, which when applied to $\bar{q}$ yields the elastic force on dm, $\bar{f}$ represents the gravitational force per unit mass, and $\bar{e}$ represents the external and control forces on dm.

After substitution of the values for the integrals into Equation (12) and rearrangement of the terms, the generic mode equations are obtained in the following form:[5,6]

$$\ddot{A}_n + \omega_n^2 A_n + \phi_n/M_n + \sum_{m=1}^{\infty} \phi_{mn}/M_n = [g_n + \sum_{m=1}^{\infty} g_{mn} + E_n]/M_n \qquad (13)$$

where A_n, ω_n, ϕ_n and M_n are the n^{th} modal amplitude, frequency, shape functions and modal mass, respectively.

g_n the effect of gravity on the n^{th} mode

E_n the effect of control and external forces on the n^{th} node

g_{mn} the coupling effect of gravity from the m^{th} mode on the n^{th} mode

ϕ_{mn} the coupling effect of elastic forces from the m^{th} mode on the n^{th} mode

V. Control of the Orbiting SCOLE with the First Four Modes Included

This model of the SCOLE is assumed to be controlled through the three torquers on the Shuttle and the six actuators located by pairs at $z = -L/3$; $z = -2L/3$ on the mast: and at G_1, the mass center of the reflector (Fig. 1). The pairs of actuators are arranged in such a manner that one acts along the x direction and the other in the y direction. The actuators, when activated to provide vibration control to the mast, will develop torques about the Orbiter center of mass. Each actuator provides a maximum of $F_x = F_y = 800$ lb.[1] force; the resulting torque contributed by all six actuators is computed as

$$\vec{T}_1 = F_y L (v_{1y}/3 + 2 v_{2y}/3 + v_{3y}) \hat{i} - F_x L (v_{1x}/3 + 2v_{2x}/3 + v_{3x})\hat{j} - (YF_x v_{3x} - XF v_{3y})\hat{k} \qquad (14)$$

This is added to the torques provided by the Shuttle's three torquers: $\bar{T}_2 = M_x U_x \hat{i} + M_y U_y \hat{j} + M_z U_z \hat{k}$, where $M_x = M_y = M_z = 10{,}000$ ft.-lb.[1] to yield the total available control torque for the system as:

$$\vec{T} = [M_x U_x + F_y L (v_{1y}/3 + 2v_{2y}/3 + v_{3y})]\hat{i} + [M_y U_y - F_x L(v_{1x}/3 + 2v_{2x}/3 + v_{3x})]\hat{j} + [M_z U_z + X F_y v_{3y} - Yv_{3x} F_x]\hat{k} \qquad (15)$$

with the control and global state vectors, respectively, chosen as

$$U = [v_{1x}, v_{1y}, v_{2x}, v_{2y}, v_{3x}, v_{3y}, u_x, u_y, u_z]^T$$

and $X = [\eta_1, \eta_2, \eta_3, A_1, A_2, A_3, A_4, \dot{\eta}_1, \dot{\eta}_2, \dot{\eta}_3, \dot{A}_1, \dot{A}_2, \dot{A}_3, \dot{A}_4]^T$

with $||v_{ix}|| \leq 1$; $||v_{iy}|| \leq 1$; and $||u_{x\leftrightarrow y}|| \leq 1$, v_{ix} represents the force due to the i^{th} actuator in the x direction and similarly for v_{iy}, i = 1,2,3. The control influence and the system state matrices are obtained, respectively as:

$$B = \begin{bmatrix} 0 & 0 \\ 7x6 & \\ \hline B_1(F,L,X,Y) & B_2(M_x,M_y,M_z) \quad 3x3 \\ \hline & 0 \\ B_3\ 4x6 & 4x3 \end{bmatrix}_{14x9} \quad (16)$$

$$A' = \begin{bmatrix} 0 & 0 & I_3 & 0 \\ 0 & 0 & 0 & I_4 \\ A_1 & A_2 & A_3 & A_4 \\ A_5 & A_6 & A_7 & 0 \end{bmatrix}_{14x14} \quad (17)$$

The specific submatrices are explicitly defined in terms of the SCOLE parameters in Ref. 5.

Here, a control, U, which minimizes the performance index

$J = \int_0^\infty (X^TQX + U^TRU)\,dt$ is obtained after using the ORACLS[7] package to solve the steady state Riccati matrix equation.

The equations describing the closed-loop systems, $\dot{X} = A'X + BU$ have been numerically integrated and the corresponding mathematical model simulated for

$$Q = \text{diag. } [5x10^6, 5x10^6, 5x10^6, 5x10^4, 5x10^4, 5x10^4, 5x10^4, 10, 10, 10, 10, 10, 10, 10]$$

and R as diag. [10,10,10,10,10,10,1,1,1]

Since both position and rate feedback of the Shuttle rotational motion and beam elastic motion will be utilized it is logical to place a greater penalty on the position displacements. Also, since the roll (and to some extent the pitch) are easier to excite than some of the elastic motions it seems intuitively correct to relax the penalty of the Shuttle control inputs as contrasted with the remaining control penalty elements.

The transient responses to some initial perturbations, confirm the controllability of the flexible SCOLE system. During the simulation of this model, the three variational attitude angles (roll, pitch, and yaw) are each subjected to a 6° single axis displacement. For each case, the effects of such displacements on the modal amplitudes of the first four modes are studied.

The largest disturbance in the flexible modes, caused by an attitude variation is observed during the roll axis maneuver (Figs. 2-5); the first mode is the most excited; its amplitude doesn't exceed 0.13 ft. (0.1% of L). All the transients are damped out within 25 seconds, largely due to the contribution of the additional 2 pairs of actuators located on the mast at $z_1 = -L/3$ and $z_2 = -2L/3$. During this response the reflector "y" axis actuator provides a maximum of 210 lb. while the forces in the two "y" actuators located a $z = -2L/3$ and $z = -L/3$, reach 120 to 80 lb, respectively. The Shuttle, "x" torquer provides a maximum of 280Ft.-lb torque bringing to 52,500 ft.-lb the maximum value of the x component of the composite control torque required for this maneuver.

In turn, the first flexible mode was given an initial amplitude equal to 1.0% of L, to stay within the linear range, Figs. 6-7 show the transient responses. Also depicted is the result of intraflexible modal coupling (Fig. 6). For this control strategy, the disturbance in the flexible mode, for the initial conditions considered herein, is damped in 15 seconds while its effect on the attitude angles takes almost 25 seconds to disappear.

VI. Conclusions

1. The SCOLE system, with gravity-gradient torques included in its open-loop dynamics, is unstable. This is due to the inertia distribution of the system in the particular configuration where the Shuttle roll axis nominally follows the orbit.

2. In the absence of control forces and torques, the system will oscillate about an equilibrium position biased from the Shuttle's symmetry axes. This phenomenon is due principally to the offset of the beam attachment to the reflector from the reflector's mass center.

3. A robust control law based on the linear regulator theory can be implemented for station keeping with maximum control efforts significantly below saturation levels.

References

1. Taylor, L.W. and Balakrishnan, A.V., "A Laboratory Experiment Used to Evaluate Control Laws for Flexible Spacecraft ... NASA/IEEE Design Challenge," Proceedings of the Fourth VPI&SU Symposium on Dynamics and Control of Large Structures, Blacksburg, Va., June 1983.

2. Montgomery, Raymond C., "COFS II Project Overview and Strawman," Control of Flexible Structures Workshop, NASA Langley Research Center, Hampton, Va., August 27-28, 1985.

3. Robertson, D.K., "Three-Dimensional Vibration Analysis of a Uniform Beam with Offset Inertial Masses at the Ends," NASA TM-86393, September 1985.

4. Mantion, M., Problemes de Mecanique Analytique, Vuibert Universite, 75005 Paris, France, 1981

5. Bainum, Peter M., et al, "The Dynamics and Control of Large Flexible Space Structures-X," Final Report Part II, NASA Grant NSG-1414, Supplement 9, Howard University, Washington, D.C. 20059, January 1988.

6. Santini, P., "Stability of Flexible Spacecrafts," Acta Astronautica, Vol. 3, 1976, pp. 685-713.

7. Armstrong, E.S., ORACLS Design System for Linear Multivariable Control, Control and Systems Theory, Vol. 10, Marcel Dekker, Inc., New York, 1980.

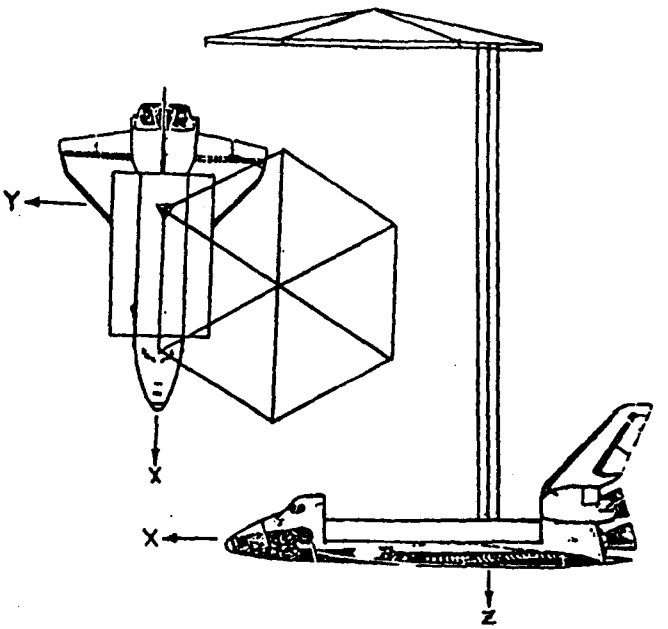

Fig. 1 Spacecraft Control Laboratory Experiment Configuration (SCOLE)

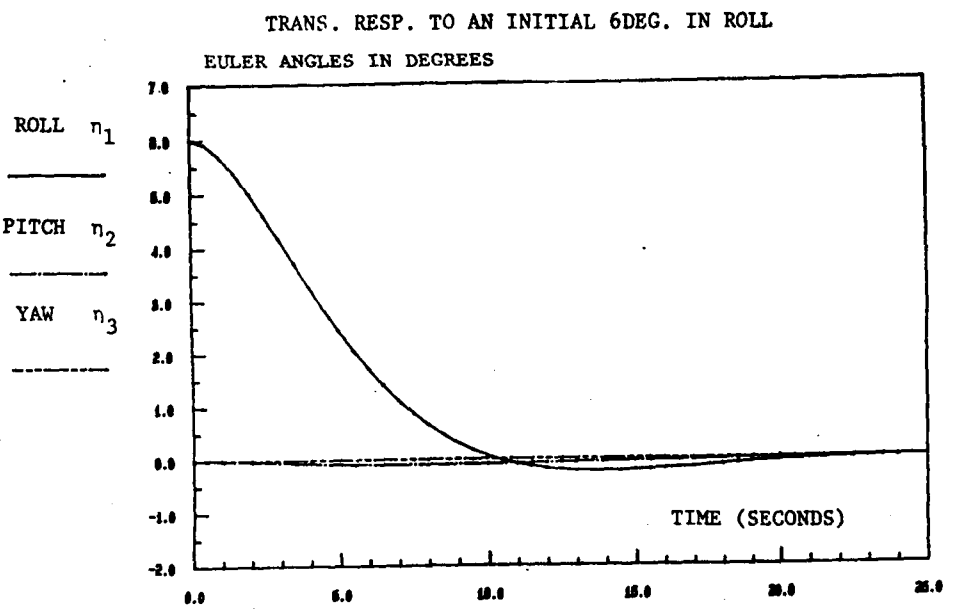

Fig. 2 Linear Model of Scole with Flexibility

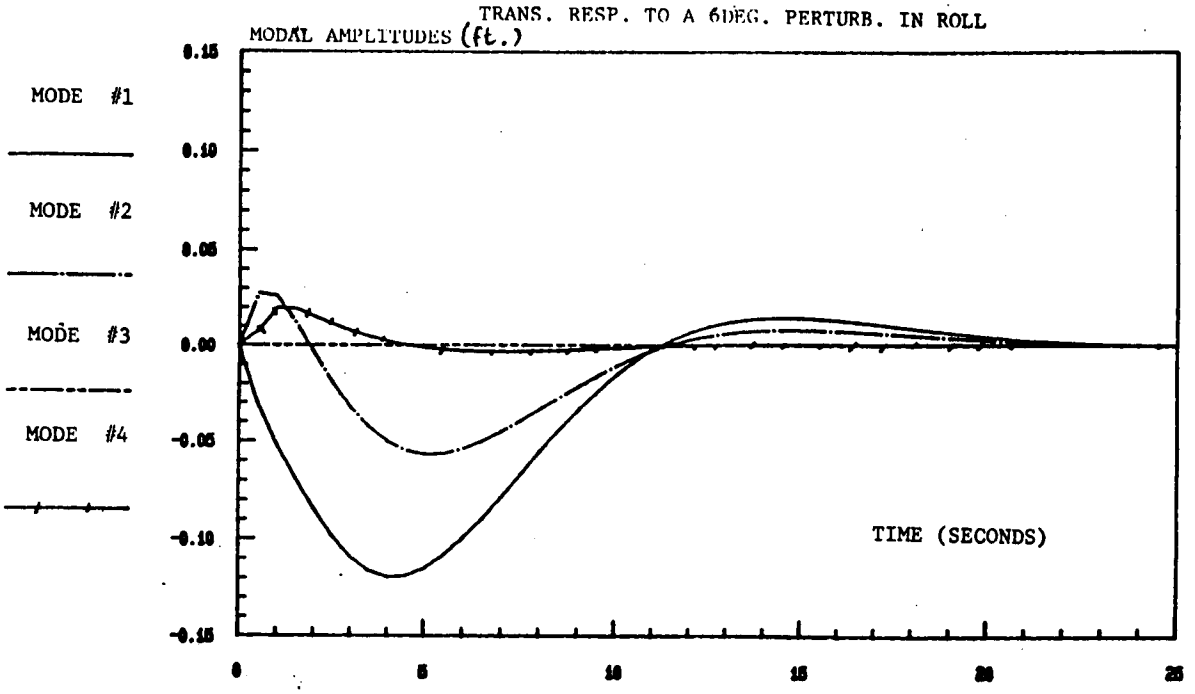

Fig. 3 Linear Model of SCOLE with Flexibilty

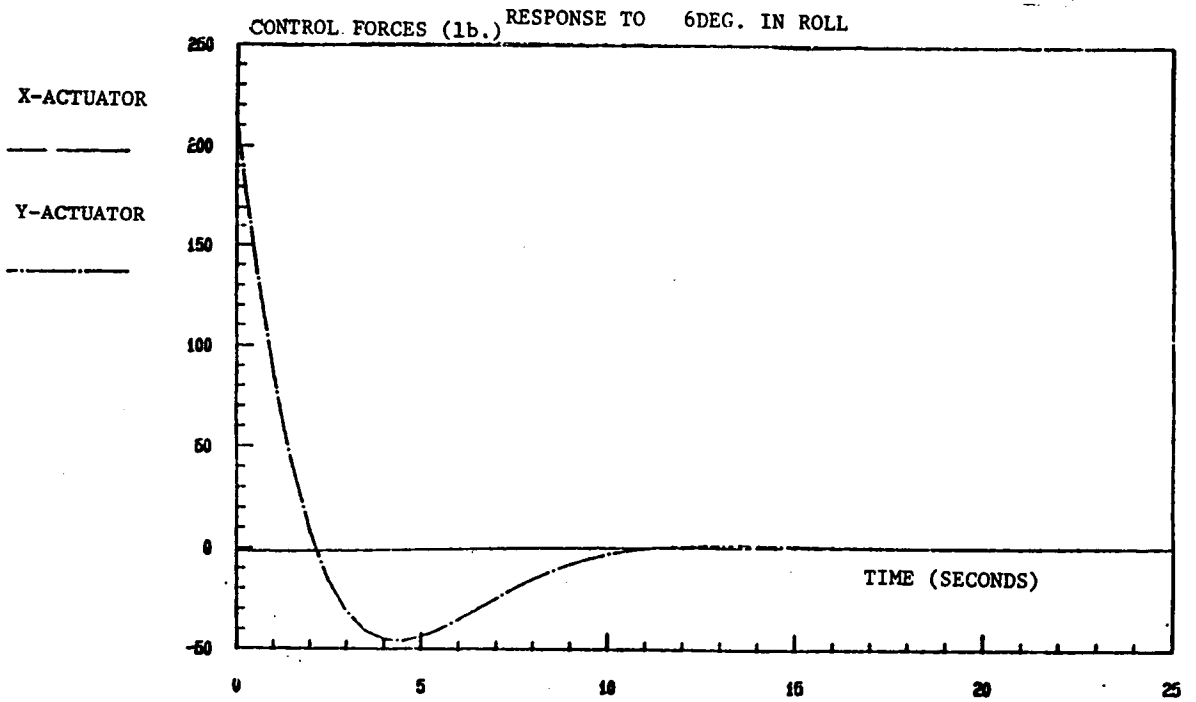

Fig. 4. Linear Model of SCOLE with Flexibility

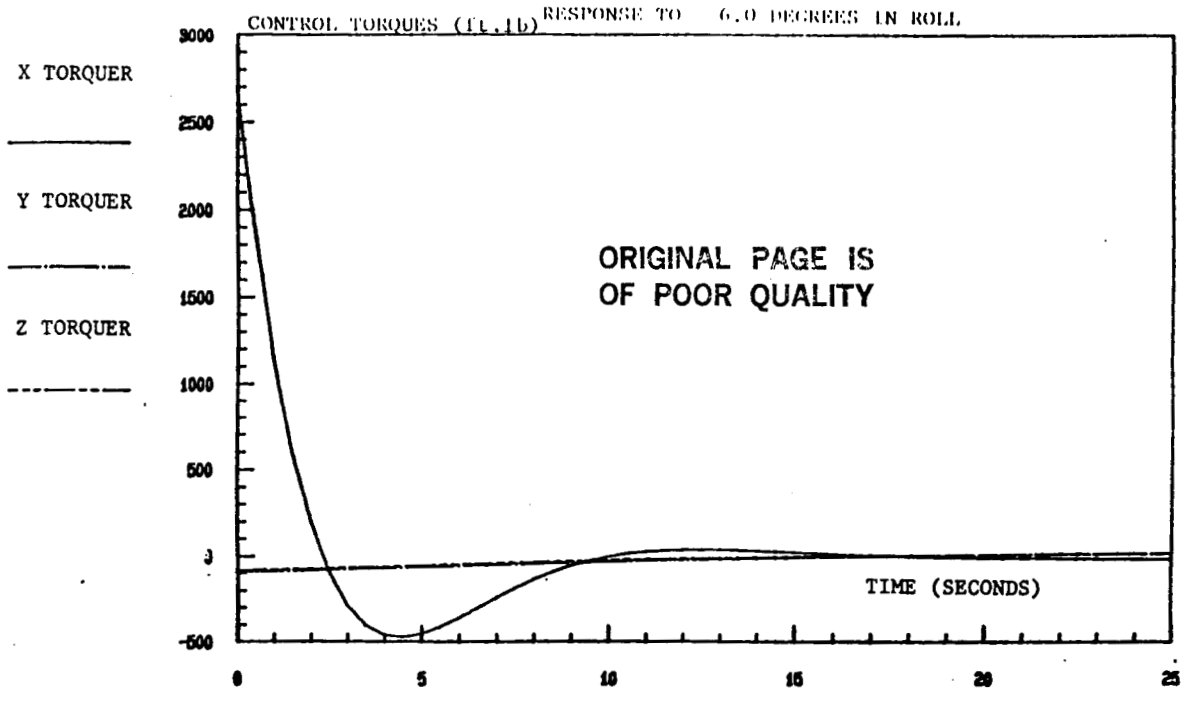

Fig. 5 Linear Model of SCOLE with Flexibility

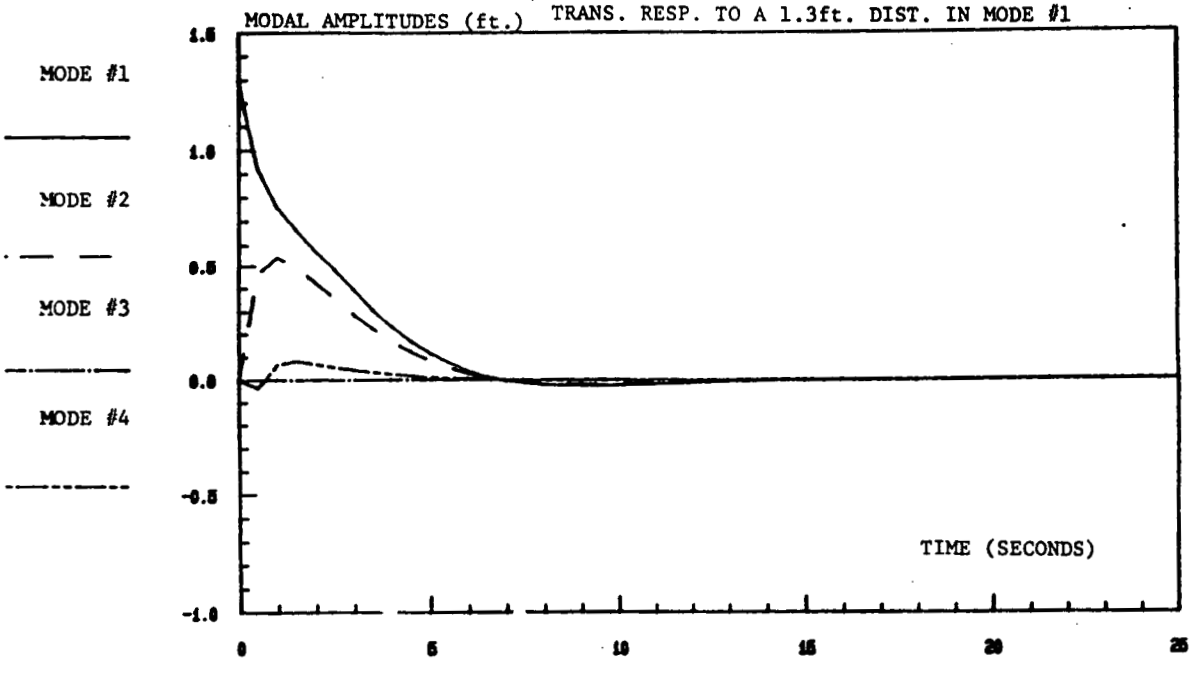

Fig. 6 Linear Model of SCOLE with Flexibility

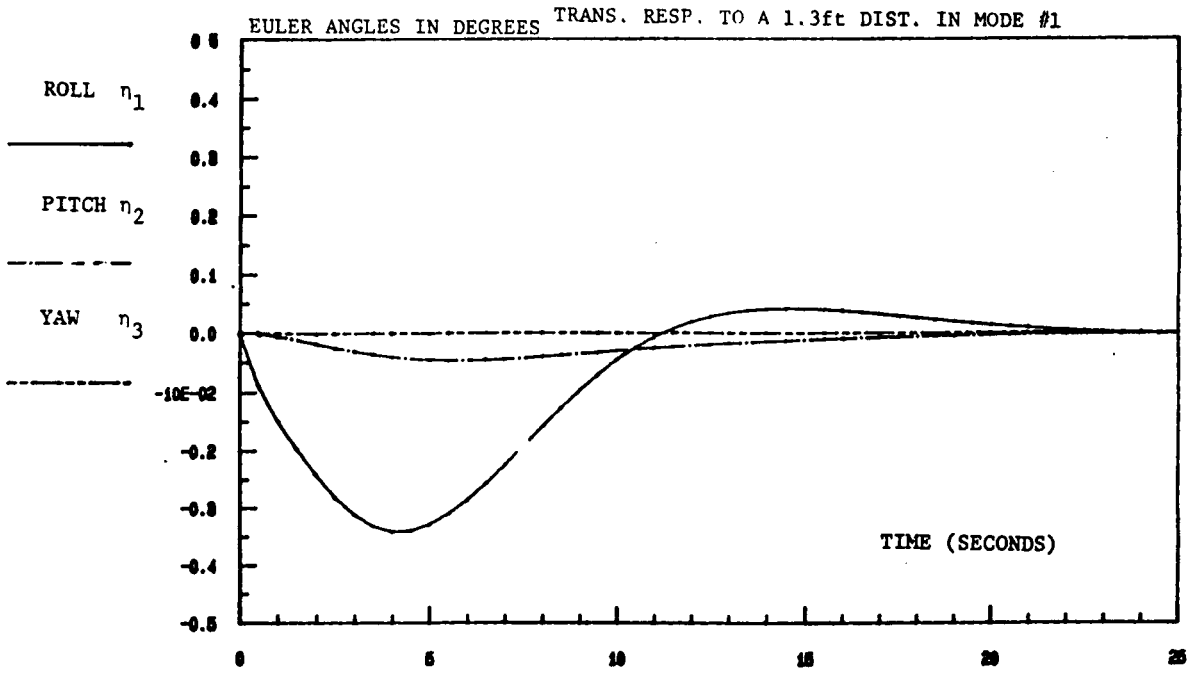

Fig. 7 Linear Model of SCOLE with Flexibility

III. RAPID SLEWING OF THE ORBITING SPACECRAFT CONTROL LABORATORY EXPERIMENT (SCOLE) USING LQR TECHNIQUES

Abstract

The rotational equations of motion, describing the dynamics of the (rigidized) proposed orbiting Spacecraft Control Laboratory Experiment during the station keeping phase, are derived using the Eulerian formulation. When the attitude angles (roll, pitch, and yaw) are assumed small, a stability analysis is conducted for the system. It is seen that the pitch equation decouples from the roll and yaw equations when the interface between the mast on the reflector is not offset or the offset is only along the Shuttle roll axis. When a second offset is introduced along the pitch axis the system and when the gravity-gradient torques are present in the dynamics, the system assumes a new equilibrium position. The linear regulator theory is used to derive a control law for the linear model of the rigidized SCOLE. This law is applied to the nonlinear model of the same configuration of the system and preliminary single axis slewing maneuvers (20° amplitude) are simulated.

I. Introduction

In several versions of a recent paper, SCOLE[1] (Spacecraft Control Laboratory Experiment), Lawrence W. Taylor, Jr. and A.V. Balakrishnan have described the ground based experimental program which is to be used to test techniques derived for active control of flexible space structures. It is a laboratory experiment based on a model of the Shuttle connected to a flexible beam with a reflecting grillage mounted at the end of the beam (Figure 1). The interface connecting point between the reflector grillage and the beam is offset in two cartesian directions with respect to the center of mass of the reflector. As a part of the design challenge, the authors stressed the need to directly compare competing control design techniques and discussed the feasibility of the such direct comparison. The challenge consists in slewing the aforementioned model line of sight through 20° in minimum time.

Based on the equations describing the motion of the SCOLE system, provided in reference 1, the expression for the reflector line of sight (LOS) error was expanded analytically and studied carefully.[2] The results showed that the SCOLE's LOS error is independent of the Euler yaw attitude angle so, only two, instead of originally three, angular parameters were needed to be concerned with in designing the pointing slew maneuvers. It was also suggested that a two stage control strategy which would first slew the whole system, as if rigid and then damp out the residual undesired mast vibrations, is most appealing. The numerical simulation test results of Reference 2 indicated that the single axis bang-bang or bang-pause-bang slew maneuvers work fairly well for pointing the LOS of SCOLE. The best pointing accuracy and shortest slew time were attained when using the Shuttle torques and the actuators placed on the reflector while imposing a 5 degree/second slew rate limit on the design.

In the present study, a mathematical model of the SCOLE system is developed assuming: the Shuttle, the mast, and the reflector to all be rigid. This development is based on the Eulerian approach. The technique consists in isolating an elemental mass of the system and deriving its angular momentum taken at the mass center of the Orbiter.[3] The expressions obtained for the elemental masses of the components of the system are integrated over the mass of the entire system to yield its angular momentum about the center of the Orbiter. The time derivative of the system angular momentum is then equated to the gravity-gradient torques[4] of the system about the same point. Such a vectorial equation, when projected along the three axes of rotation, yields the system rotational equations of motion. These equations are then linearized to yield a model which provides the basis for the control law synthesis developed in this study.

II. Development of Equations of Motion

The rotational equations of motion for the system will be derived by taking the time derivative of the angular momentum of the system at G, the center of mass of the Shuttle, and by equating it to the external torques applied to the system.

A. Angular Momentum of the Shuttle about its Mass Center, G.

The angular momentum of the Shuttle, taken as a rigid body, about its center of mass, G is

$$\bar{H}_{S/G} = \bar{\bar{I}}_{S/G}\, \bar{\Omega}_{S/R_0} \qquad (1)$$

where $\bar{\bar{I}}_{S/G}$ is the inertia tensor, with elements I_{si}, of the Shuttle and $\bar{\Omega}_{S/R_0}$, the Shuttle's inertial angular velocity, with components Ω_i, $i = x,y,z$, along the Shuttle's symmetry axes.

B. Anuglar Momentum of the Rigid Beam about G

The angular momentum of the beam about the Shuttle mass center, G, can be expressed as

$\vec{H}_{M/G} = \bar{\bar{I}}_{M/G}\,\bar{\Omega}_{R_0}$ where $\bar{\bar{I}}_{M/G}$ is the inertia tensor of the beam transferred at G, using the parallel axis theorem.

$$\vec{H}_{M/G} = -\frac{ML^2}{3}(\Omega_x \hat{i} + \Omega_y \hat{j}) \qquad (2)$$

where M is the mass of the beam whose length is L.

C. Angular Momentum of the Reflector about G

Since here the beam is considered rigid, the reflector can be assumed to be located at a constant distance from G.

Using the transfer theorem[3] for the angular momentum, the angular momentum, $\vec{H}_{R/G}$, of the reflector, assumed rigid, about G can be expressed as:

$$\vec{H}_{R/G} = \bar{\bar{I}}_{R/G_1}\,\bar{\Omega}_{R/R} + M_R\,\overline{GG_1} \times \frac{d}{dt}(\vec{GG_1})\Big|_{R_0} \qquad (3)$$

where I_{R/G_1}, the inertia tensor of the reflector expressed at G_1, its center of mass, and $\bar{\Omega}_{R/R_0} = \bar{\Omega}_{S/R}$ (where $\bar{\Omega}_{R/R_0}$ is the inertial angular velocity of the reflector.

D. Angular Momentum of the System about G

The angular momentum of the system about G, $\vec{H}_{syst/G}$, is given by the sum of the angular momentum of each of the three components evaluated about the same point, G:

$$\vec{H}_{syst/G} = \vec{H}_{S/G} + \vec{H}_{M/G} + \vec{H}_{R/G}$$

$$\text{or} \quad \vec{H}_{syst/G} = \vec{H}_x \hat{i} + \vec{H}_y \hat{j} + \vec{H}_z \hat{k} \qquad (4)$$

E. Rotational Equations of Motion (Torque Free)

The rotational equations of motion for the system, when free of all external torques, are obtained as:

$$\frac{d}{dt}(\vec{H}_{syst/G})\Big|_{R_0} = \dot{\vec{H}}_{syst/G/R} + \vec{\Omega}_{S/R_0} \times \vec{H}_{syst/G} = \vec{0} \qquad (5)$$

The vector equation (5) itself is equivalent to

$$\begin{aligned}
&\dot{H}_x + \Omega_y H_z - \Omega_z H_y = 0\\
&\dot{H}_y + \Omega_z H_x - \Omega_x H_z = 0\\
&\dot{H}_z + \Omega_x H_y - \Omega_y H_x = 0
\end{aligned} \qquad (6)$$

III. Stability of the SCOLE in some of its Configurations

Equations (6) describe the torque-free nonlinear dynamics of the SCOLE configuration. In what follows, the stability analysis of the "rigidized" SCOLE system will be conducted in three different steps for the cases where the Shuttle's roll, pitch, and yaw displacement amplitudes (ψ,θ,ϕ respectively) are assumed small.

First, it will be assumed that the interface point between the beam and the reflector is the reflector center of mass; second, still assuming, the mast rigid, the interface point will be offset in the "X" direction; finally, a two dimensional offset of the interface point will be introduced. The mast will still be assumed rigid. The system dynamics, in all the aforementioned cases, includes the gravity-gradient torques.[4]

A. The SCOLE System without Offset.

In the absence of offset in the location of the interface point (X=Y=0), with gravity-gradient torques present in the system, Equations (6) can be rewritten as[5]:

$$\begin{aligned}
&\ddot{\psi}[I_{S_1} + ML^2/3 + M_R L^2 + I_{R_1}] - \ddot{\phi} I_{S_4} - \omega_0 \dot{\phi}[-I_{S_2} + I_{S_3}\\
&+ I_{S_1} + I_{R_1} - I_{R_2} + I_{R_3}] - \omega_0^2 \phi I_{S_4} - \omega_0^2 \psi[I_{S_3} - I_{S_2}\\
&+ I_{R_3} - I_{R_2} - ML^2/3 - M_R L^2 + 3(I_3 - I_2)] = 0
\end{aligned} \qquad (7)$$

$$\ddot{\theta}\,[I_{S_2} + I_{R_2} + M_R L^2 + ML^2/3] + 3\omega_0^2 \theta (I_1 - I_3) + 3\omega_0^2 I_4 = 0 \qquad (8)$$

$$\begin{aligned}
&-\ddot{\psi}\, I_{S_4} + \ddot{\phi}\,(I_{S_3} + I_{R_3}) + \omega_0 \dot{\psi}\,[I_{S_1}\\
&+ I_{S_3} - I_{S_2} + I_{R_1} + I_{R_3} - I_{R_2}] - \omega_0^2 \phi[I_{S_1} - I_{S_2}\\
&+ I_{R_1} - I_{R_2}] - \omega_0^2 \psi[I_{S_4} + 3I_4] = 0
\end{aligned} \qquad (9)$$

where I_4 is the Shuttle's xz product of inertia and $I_{1,2,3}$ the composite system inertias with respect to the Shuttle axes. It is seen that in such a configuration, in the linear range, the equation describing the pitch motion (Equation (8)) of the system decouples from the equations describing the motion in the two remaining degrees of freedom (Equations (7) and (9)).

Equation (8) can be recast in the following form:

$$\ddot{\theta} h_1 - \theta h_2 + h_3 = 0 \qquad (10)$$

in which,

$$h_1 = I_{S_2} + I_{R_2} + M_R L^2 + \frac{ML^2}{3}$$

$$h_2 = 3\omega_0^2 (I_3 - I_1) \text{ and } h_3 = 3\omega_0^2 I_4$$

The homogeneous part of Equation (10) yields the following solution:

$$\theta_h = C_1 e^{\delta t} + C_2 e^{-\delta t}$$

where $\delta = \sqrt{h_2/h_1}$

since for this configuration, $h_2/h_1 > 0$, $\theta_h(t)$ is unstable. Thus, in the absence of control, the system is seen to be unstable in its pitch degree of freedom.

Equations (7) and (9) which have the following forms, respectively,

$$\ddot{\psi}k_1 + \ddot{\phi}k_2 - \dot{\phi}k_3 + \phi k_4 - \psi k_5 = 0$$

$$\ddot{\psi}n_1 + \ddot{\phi}n_2 + \dot{\psi}n_3 - \phi n_4 + \psi n_5 = 0$$

can be recast in the following state matrix format:

$$\begin{bmatrix} \dot{\psi} \\ \dot{\phi} \\ \ddot{\psi} \\ \ddot{\phi} \end{bmatrix} = \begin{bmatrix} 0 & 0 & 1 & 0 \\ 0 & 0 & 0 & 1 \\ P_2 & P_4 & P_1 & P_3 \\ -P_6 & -P_8 & -P_5 & -P_7 \end{bmatrix} \begin{bmatrix} \psi \\ \phi \\ \dot{\psi} \\ \dot{\phi} \end{bmatrix}$$

Some of the eigenvalues of the state matrix, in this subcase have positive real parts, based on the actual SCOLE system parameters indicating instability in the open loop dynamics of the roll and yaw degrees of freedom.

B. The SCOLE System with Offset in the "X" Direction

The configuration analyzed in the previous section is upgraded to the one considered here by letting X be non-zero in the equations of motion (6) and by setting the "Y offset" equal to zero.

The equations of motion then become:

$$\ddot{\psi}[I_{S_1} + ML^2/3 + M_R L^2 + I_{R_1}]$$
$$-\ddot{\phi}(I_{S_4} + M_R XL) - \dot{\phi}\omega_0[I_{S_1} + I_{S_3} - I_{S_2}$$
$$+I_{R_1} + I_{R_3} - I_{R_2}] - \omega_0^2\phi(I_{S_4} + M_R XL) - \omega_0^2\psi[I_{S_3}$$
$$- I_{S_2} - \frac{ML^2}{3} + I_{R_3} - I_{R_2} - M_R L^2 + 3(I_3' - I_2')] = 0 \quad (11)$$

$$\ddot{\theta}\,[I_{S_2} + I_{R_2} + M_R(X^2+L^2) + \frac{ML^2}{3}] + 3\omega_0^2\theta\,(I_1' - I_3')$$
$$+ 3\omega_0^2(I_{S_4} + M_R XL) = 0 \quad (12)$$

$$-\ddot{\psi}\,[I_{S_4} + M_R XL] + \ddot{\phi}\,[I_{S_3} + I_{R_3} + M_R X^2]$$
$$+ \omega_0\dot{\psi}[I_{S_1} - I_{S_2} + I_{S_3} + I_{R_1} + I_{R_3} - I_{R_2}]$$
$$- \omega_0^2\phi\,[I_{S_1} - I_{S_2} + I_{R_1} - I_{R_2} - M_R X^2]$$
$$- \omega_0^2\,\psi\,\{3(I_{S_4} + M_R XL)\} = 0 \quad (13)$$

where I_i represent the composite inertias about the Shuttle axes for this case and ω_0 is the (circular) orbital angular velocity.

Again, it is seen that in this configuration, the pitch equation, (Equation 12), decouples from the roll, (Equation II)) and yaw (Equation 13)) equations and can be rewritten as:

$$\ddot{\theta}h_1' - \theta h_2' + h_3' = 0 \quad (14)$$

where, $h_1' = I_{S_2} + I_{R_2} + M_R(X^2 + L^2) + ML^2/3$

$h_2' = 3\omega_0^2(I_3' - I_1')$; and $h_3' = 3\omega_0^2(I_{S_4} + M_R XL)$

Here again, h_2/h_1 is a positive quantity. By analogy with the previous configuration,

$$\theta(t) = \theta_0 \cosh \delta' t + \frac{\dot{\theta}_0}{\delta'} \sinh \delta' t + h_3'/h_2' (1 - \cosh \delta' t) \quad (15)$$

with

$$\delta' = \sqrt{h_3'/h_1'}$$

In the absence of control, it is seen that the pitch angle is unbounded indicating an instability in that degree of freedom.

A reasoning similar to the one previously done for the case without offset, enables one to recast Equations (11) and (13) in the following state matrix format:

$$\dot{X} = A' X \quad \text{or}$$

$$\begin{bmatrix} \dot{\psi} \\ \dot{\phi} \\ \ddot{\psi} \\ \ddot{\phi} \end{bmatrix} = \begin{bmatrix} 0 & 1 & 1 & 0 \\ 0 & 0 & 0 & 1 \\ P_2' & P_4' & P_1' & P_3' \\ -P_6' & -P_8' & P_5' & -P_7' \end{bmatrix} \begin{bmatrix} \psi \\ \phi \\ \dot{\psi} \\ \dot{\phi} \end{bmatrix} \quad (16)$$

p_i', $i = 1 \to 8$ are defined in terms of the k_i' and n_i' similar to the case without offset, and appropriate k_i', n_i' now include the effects of the X offset.[5] Here again it is seen that some of the eigenvalues of the state matrix, A', have positive real parts. Therefore, the open loop dynamics of the system are seen to be unstable in its roll and yaw degrees of freedom.

C. The SCOLE System with Offset in Both the "X" and "Y" Directions

If once more the description of the system dynamics is upgraded by introducing the "Y offset", the rotational equations of motion become:

$$\ddot{\psi}[I_{S_1} + I_{R_1} + \frac{ML^2}{3} + M_R(L^2 + Y^2)] - \ddot{\phi}I_{xz}$$

$$-\ddot{\theta}M_R XY - \dot{\phi}\omega_0[I_{S_1} + I_{S_3} + 2M_R Y^2 - I_{S_2} + I_{R_1} + I_{R_3}$$

$$-I_{R_2}] - \omega_0\dot{\theta}M_R YL - \omega_0^2\psi[I_{S_3} - I_{S_2} + I_{R_3} - I_{R_2}$$

$$+M_R(Y^2 - L^2) - \frac{ML}{3} + 3(I_{zz} - I_{yy})] - \omega_0^2\phi I_{xz} - 3\omega_0^2\theta I_{xy}$$

$$+\omega_0^2[M_R YL + 3I_{yz}] = 0 \qquad (17)$$

$$\ddot{\theta}[I_{S_2} + \frac{ML^2}{3} + I_{R_2} + M_R(L^2 + X^2)] + \ddot{\phi}M_R YL$$

$$+\ddot{\psi}M_R XY + \omega_0\dot{\phi}M_R XY - \omega_0\dot{\psi}M_2 YL + \omega_0^2\phi M_R YL - 3\omega_0^2\psi I_{xy}$$

$$+3\omega_0^2\theta(I_{xx} - I_{zz}) + 3\omega_0^2 I_{xz} = 0 \qquad (18)$$

$$\ddot{\phi}[I_{S_3} + I_{R_3} + M_R(X^2 + Y^2)] - \ddot{\psi}I_{zx}$$

$$+\omega_0\dot{\psi}[I_{S_1} + I_{S_3} - I_{S_2} + I_{R_1} + I_{R_3} - I_{R_2}$$

$$+2M_R Y^2] - \ddot{\theta}M_R YL - \omega_0\dot{\theta}\, M_R XY + 3\omega_0^2\theta I_{yz}$$

$$-\omega_0^2\psi(4I_{xz}) - \omega_0^2\phi[I_{S_1} - I_{S_2} + I_{R_1} - I_{R_2}$$

$$+M_R(Y^2 - X^2)] - \omega_0^2 M_R XY = 0 \qquad (19)$$

It should be noted here that the pitch equation no longer decouples from the roll and yaw equations. Equations (17), (18), (19) can be recast in the following state matrix format

$$\dot{X} = A'' X + C \text{ or}$$

$$\begin{bmatrix} \dot{\psi} \\ \dot{\theta} \\ \dot{\phi} \\ \ddot{\psi} \\ \ddot{\theta} \\ \ddot{\phi} \end{bmatrix} = \begin{bmatrix} 0 & 0 & 0 & 1 & 0 & 0 \\ 0 & 0 & 0 & 0 & 1 & 0 \\ 0 & 0 & 0 & 0 & 0 & 1 \\ a_1 & a_2 & a_3 & a_4 & a_5 & a_6 \\ a_7 & a_8 & a_9 & a_{10} & a_{11} & a_{12} \\ a_{13} & a_{14} & a_{15} & a_{16} & a_{17} & a_{18} \end{bmatrix} \begin{bmatrix} \psi \\ \theta \\ \phi \\ \dot{\psi} \\ \dot{\theta} \\ \dot{\phi} \end{bmatrix} + \begin{bmatrix} 0 \\ 0 \\ 0 \\ a_{19} \\ a_{20} \\ a_{21} \end{bmatrix} \qquad (20)$$

where, the a_i are functions of the various component inertias and the X,Y offset parameters.[5]

Since the Shuttle axes do not correspond to the principal axes of the system, the system dynamics appear in the following state form:

$$\dot{X} = A_{offset}\, X + C \qquad (21)$$

where A_{offset} = A" form Eq. (20) indicating that the system equilibrium position is no longer $\psi_0 = \theta_0 = \phi_0 = 0$.

Let ψ_e, θ_e, and ϕ_e be the equilibrium position for this configuration of the system. Then,

$$\psi = \psi_e + \eta_1 \text{ and } \dot{\psi} = \dot{\eta}_1$$

$$\theta = \theta_e + \eta_2 \qquad \dot{\theta} = \dot{\eta}_2$$

$$\phi \quad \phi_e + \eta_3 \qquad \dot{\phi} = \dot{\eta}_3$$

The new state vector is $[\eta_1, \eta_2, \eta_3, \dot{\eta}_1, \dot{\eta}_2, \dot{\eta}_3]^T$. Also ψ_e, θ_e, and ϕ_e satisfy

$$a_1\psi_e + a_2\theta_e + a_3\phi_e = a_{19}$$

$$a_7\psi_e + a_8\theta_e + a_9\phi_e = a_{20}$$

$$a_{13}\psi_e + a_{14}\theta_e + a_{15}\phi_e = a_{21}$$

and this simultaneous system can be solved to determine ψ_e, θ_e, ϕ_e.

After substituting the new state vector in the equations describing the system dynamics, linearizing them about the new equilibrium position, recasting them into a state format, one arrives at $[\dot{\eta}_i] = [A_{new}]\,[\eta_i]$. The real parts of three of the new state matrix eigenvalues are found here to be positive indicating that the open loop system in this configuration is also unstable.

IV. Control Synthesis

First, within the linear range, the motion of the rigidized SCOLE is controlled using a strategy, based on the linear regulator problem when the system is subjected to some small perturbations in its degrees of freedom; second, the control strategy derived for the linear model of the rigidized SCOLE is applied to the non-linear model of the same configuration. Preliminary slew maneuvers are tested by assuming single axis initial perturbations of 20° in the roll, pitch, and yaw degrees of freedom, respectively. The three Shuttle torquers and the two actuators on the reflector (Fig. 1) are then assumed to be the only sources of control moments. The controllers are seen not to reach saturation.

A. Control of the Linearized Model of SCOLE

During the control of this model, it is assumed that the actuators located on the mast (proof masses) are not activated. As a result, the system is controlled by means of the Orbiter torquers and the actuators located on the reflector (Fig. 1).

Since the Shuttle is equipped with three torquers acting about the x,y, and z directions, the total control torque available can be written as

$$\vec{T} = \{M_x U_x + 130F_y v_y)\,\hat{i} + (M_y U_y - 130\, F_x v_x)\hat{j}$$

$$+ (M_z U_z + 32.5F_x v_x + 18.75F_y v_y)\hat{k}\} \text{ ft.-lb}$$

with the limits for M_x, M_y and M_z = 10,000. ft. lb; F_x and F_y = 800 lb.[1] The constraints, therefore, are

$$|U_x| \leq 1;\ |U_y| \leq 1;\ |U_z| \leq 1;\ |v_x| \leq 1;\ \text{and}$$

$$|v_y| \leq 1$$

where U, the control vector is expressed as

$U = [v_1, v_2, U_1, U_2, U_3]^T$, while the control influence matrix can then be written as:

$$B = \begin{bmatrix} 0 & 0 & 0 & 0 & 0 \\ 0 & 0 & 0 & 0 & 0 \\ 0 & 0 & 0 & 0 & 0 \\ 0 & 130F_y & M_x & 0 & 0 \\ -130F_x & 0 & 0 & M_y & 0 \\ 32.5F_x & 18.75F_y & 0 & 0 & M_z \end{bmatrix}$$

The optimal control U which minimizes a performance index

$$J = \int_0^\infty (X^TQX+U^TRU)\, dt$$

is given by

$$U = -KX = -(R^{-1}B^TP)X$$

where P is the positive definite solution of the steady state Ricatti matrix equation.[6] The equations describing the closed loop system can be recast in the following matrix format:

$$\dot{X} = AX + BU$$

where $A = A_{new}$ and $X = [\eta_1, \eta_2, \eta_3, \dot{\eta}_1, \dot{\eta}_2, \dot{\eta}_3]^T$ from the discussion following Eq. (20). After substitution of -KX for U, the closed loop equation can be rewritten as

$$\dot{X} = (A-BK)X$$

A parametric study was conducted by first examining the variation of the real part of the least damped mode as a function of different values for the (assumed) diagonal Q and R weighting elements (Figure 2). In this initial study, each of the diagonal Q elements were assumed equal i.e. Q=diag. [SQ] and also each of the diagonal R elements were assumed equal R = diag. [SR]. Figure 2 corresponds to a model of the rigidized SCOLE system where the dimensionality of the state vector is 6 x 1 and 3 Shuttle torquers plus 2 reflector actuators describe the control inputs.

It can be seen from Fig. 2 that the best closed-loop transient results are obtained from using larger values of the state penalty along with smaller values of the control penalty elements. However, when the closed loop dynamic responses were simulated using the best combinations of Q and R it was seen that some of the controllers reached saturation levels for responses with initial conditions on pitch, roll, and yaw taken within the slewing angle range (i.e. approx. 0.3 rad.).

As an alternative, the concept of split weighting of both the state and control penalty elements was considered, initially for the rigidized SCOLE model. Since the roll (and to some extent also the pitch) are easier motions to excite than the yaw, due to the SCOLE moment of inertia distribution, it seems intuitively correct to relax the penalty of these control inputs as contrasted with the remaining control penalty elements. Also since both position and rate feedback of the Shuttle rotational motion will be utilized, it appears logical to place a far greater penalty on the (angular) position displacements. Based on this philosophy and by trial and error, the set of Q and R which produced the largest absolute value of the real part of the least damped mode (while at the same time avoiding saturation during 20° single axis slewing maneuvers) was selected as

$$Q = \text{diag. } [5\text{x}10^{12},\ 5\text{x}10^{12},\ 5\text{x}10^{12},\ 1,\ 1,\ 1]$$

and $R = \text{diag. } [1,\ 1,\ .1,\ .2,\ 1]$

For this set of Q and R the closed log eigenvalues for the rigidized SCOLE model are calculated

$R(\lambda_i)$	$Im(\lambda_i)$
-0.431436E+02	0.431436E+02
-0.431436E+02	-0.431436E+02
-0.132023E+03	0.132023E+03
-0.132023E+03	-0.132023E+03
-0.328320E+03	0.328320E+03
-0.328320E+03	-0.328320E+03

It has been assumed here that all the state variables are available at each instant (observability matrix = I_6).

The closed loop dynamics has been simulated for transient responses to a 6° initial perturbation in roll. Figure 3 shows that a 6° perturbation in roll is damped out in approximately 13 seconds. During that single axis maneuver, it should also be noticed that the coupling disturbs the yaw degree of freedom, which reaches a maximum amplitude of 0.25° degree. Figures 3a, 3b, and 3c show, for the 6° maneuver about the roll axis, the forces required from the reflector actuators, the efforts produced by the Shuttle's torquers, and the components of the equivalent total torque acting on the SCOLE system, respectively. The reflector "y" actuator and the Shuttle's "x" torquer are the more active controllers for this maneuver, as expected.

B. Rigidized SCOLE Preliminary Slew Maneuvers

In this section, the equations governing the motion of the rigidized SCOLE, outside of the linear range, are developed from the most general rotational equations of motion previously derived. The control laws obtained from the application of the linear regulator theory to the linearized model of the rigidized SCOLE are tested for large amplitude manuevers. The closed loop system dynamics are numerically simulated. For single axis slew maneuvers about the roll, pitch, and yaw axes, respectively, the time responses for the Euler angles, the control efforts required of the reflector actuators, control torques demanded from the Shuttle's torquers, and the components of the total control moments, are depicted in the subsequent figures. This enables one to determine the margin left in which to optimize the control strategy without causing saturation of the controllers.

The equations governing the motion of the rigidized SCOLE system during large amplitude maneuvers in the presence of gravity-gradient and control torques are obtained as:

i) The Roll Equation

$$\dot{H}_x + \Omega_y H_z - \Omega_z H_y = T_x \qquad (22)$$

ii) The Pitch Equation

$$\dot{H}_y + \Omega_z H_x - \Omega_x H_z = T_y \qquad (23)$$

iii) The Yaw Equation

$$\dot{H}_z + \Omega_x H_y - \Omega_y H_x = T_z \qquad (24)$$

where T_x, T_y, and T_z are the components of the external torques acting on the system (including the control torques previously derived for the linear model of the rigidized SCOLE where the feedback now depends on the original Euler angles and their rates for maneuvers made relative to the Shuttle roll, pitch, and yaw axes).

The closed-loop system dynamics described by Equations (22), (23), and (24) have been numerically simulated and the results are shown in Figs. 4 to 7. Fig 4 shows the time responses to an initial 20° alignment in roll. It is seen that a 20° slew about the roll axis can be achieved in about 30 seconds.

For this control strategy, the single axis slew maneuver about the roll axis uses 80% of the control forces available from the corresponding actuator located on the reflector, and 80% of the control torque available from the corresponding Shuttle torquer. None of the controllers reach saturation. Also depicted in the Fig. 7 are the components of the total control moments for this case (moments of the reflector control forces taken about the Shuttle's mass center, plus moments of the Shuttle's torquers). This will make possible a comparison between this strategy and other future control laws which would be based on the two point boundary-value problem,[7] where this or combinations of control inputs may be employed. Similar results have also been simulated for slew maneuvers about the Shuttle's pitch and yaw axes.[5]

V. Conclusions

In conclusion, it is seen that: a) a control strategy derived from the linearized model of the rigidized SCOLE based on the linear regulator theory, works well when it is used for single axis slew maneuvers through amplitude angles as large as 20°. For the case of the yaw axis slew maneuver[5] (where the control effort does not benefit directly from the long moment arm provided by the mast) by suitable adjustment of the gains, it is possible to achieve a slew in approximately 100 secs. with the use of up to 90% of the Shuttle's (yaw) saturation torque. In comparison with the results of Ref. 7, where fast slews of order of 10-20 secs are accompanied by series of bang-bang type control efforts in more than one control input, the results here provide a definite trade-off between the slightly increased slew times with the considerable reduction in over-all control effort; b) the SCOLE system, with gravity-gradient torques included in its open-loop dynamics, is unstable. This is due to the inertia distribution in the particular configuration where the Shuttle roll axis nominally follows the orbit; and c) the equation describing the pitch motion decouples, within the linear range, from the roll and yaw equations, when the gravity-gradient torques effects are present in the system dynamics, and when the mast attachment point on the reflector is not offset or when the offset is parallel to the roll axis.

References

1. Taylor, L.W. and Balakrishnan, A.V., "A Laboratory Experiment Used to Evaluate Control Laws for Flexible Spacecraft . . . NASA/IEEE Design Challenge," Proceedings of the Fourth VPI&SU Symposium on Dynamics and Control of Large Structures, Blacksburg, Va., June 1983.

2. Lin, J.G., "Rapid Torque Limited Line of Sight Pointing of SCOLE (Spacecraft Control Laboratory Experiment) Configuration," AIAA Guidance, Navigation, and Control Conference, Williamsburg, Va., August 18-20, 1986, Paper No. 86-1991.

3. Mantion, M., Problemes de Mecanique Analytique, Vuibert Universite, 75005 Paris, France, 1981.

4. Santini, P., "Stability of Flexible Spacecraft," Acta Astronautica, Vol. 3, 1976, pp. 685-713.

5. Bainum, Peter M., et al, "The Dynamics and Control of Large Flexible Space Structures - X" Final Report Part II, NASA Grant NSG-1414, Supplement 9, Howard University, Washington, D.C. 20059, January 1988.

6. Armstrong, E.S., ORACLS Design System for Linear Multivariable Control, Control and Systems Theory, Vol. 10, Marcel Dekker, Inc., New York, 1980.

7. Li, F. and Bainum, P.M., "Minimum Time Attitude Slewing Maneuvers of a Rigid Spacecraft," AIAA Aerospace Sciences Meeting, Reno, Nevada, Jan. 11-14, 1988, Paper No. 88-0675.

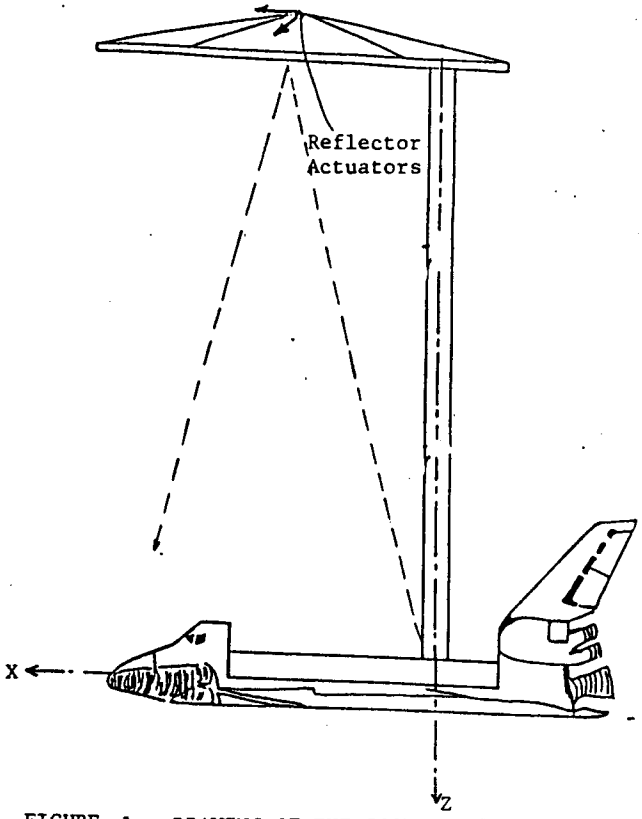

FIGURE 1: DRAWING OF THE SCOLE CONFIGURATION

FIGURE 2: REAL PART OF LEAST DAMPED MODE VS. [R]

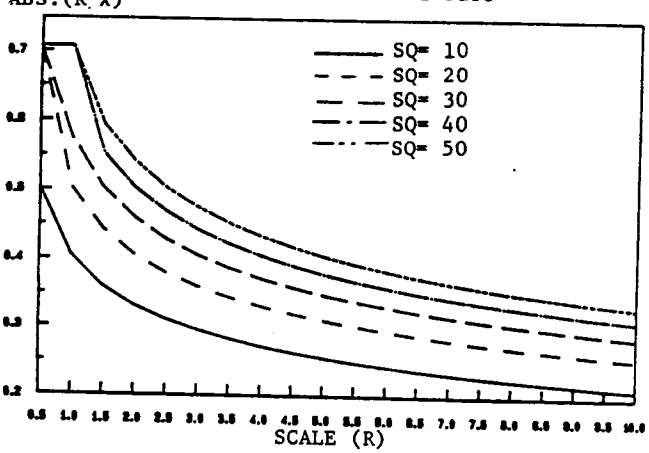

FIGURE 3 : SCOLE: TRANSIENT RESPONSES

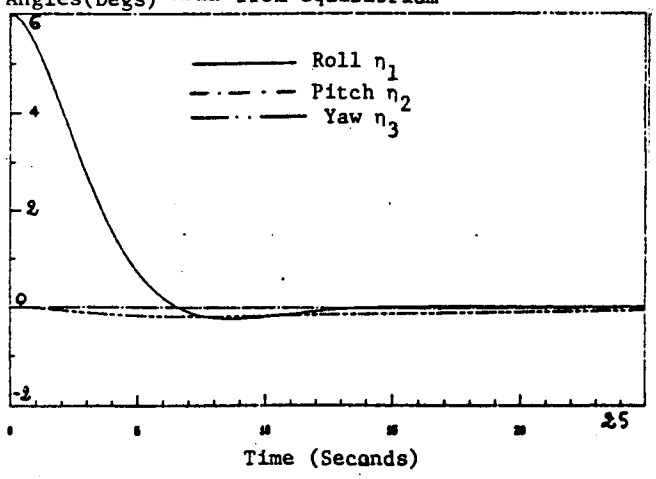

FIGURE 3a: RIGID SCOLE - CONTROL EFFORTS

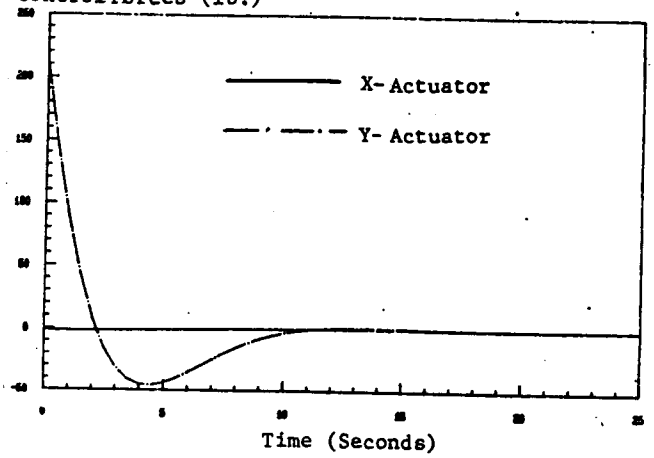

FIGURE 3b: RIGID SCOLE - CONTROL EFFORTS

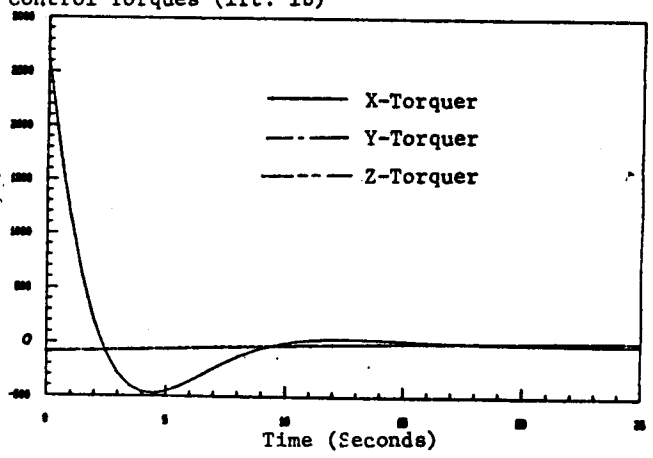

ORIGINAL PAGE IS
OF POOR QUALITY

Figure 3c: RIGID SCOLE - CONTROL EFFORTS
Response to a 6.0 Degrees in Roll

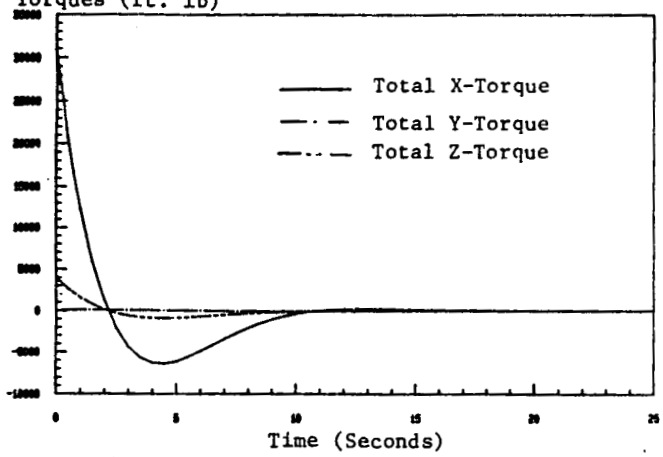

Figure 4:
SCOLE: PRELIMINARY SLEW (RIGID SCOLE)
Slew about the Roll Axis (From 20° to 0.)

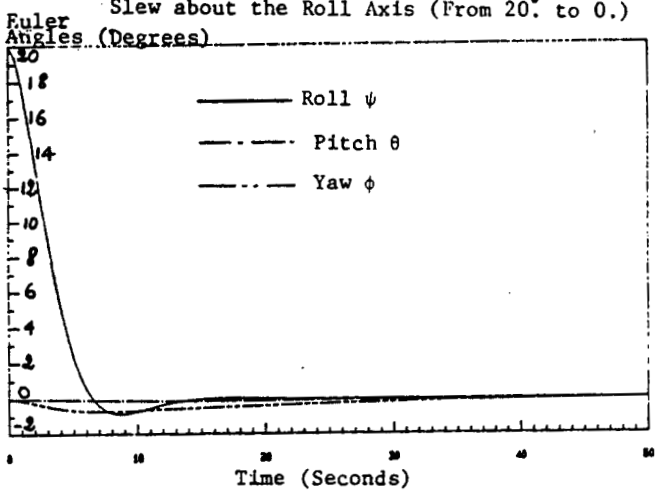

Figure 5:
SCOLE: PRELIMINARY SLEW-CONTROL EFFORTS
20.0 Degrees Slew about the Roll Axis

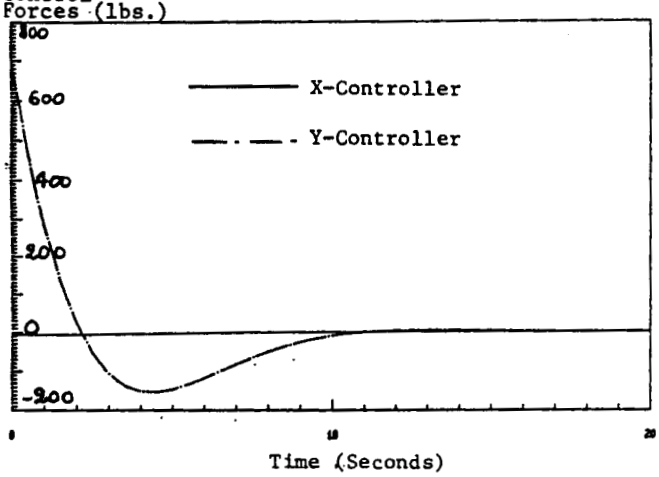

Figure 6:
SCOLE: PRELIMINARY SLEW-CONTROL EFFORTS
20.0 Degrees Slew about the Roll Axis

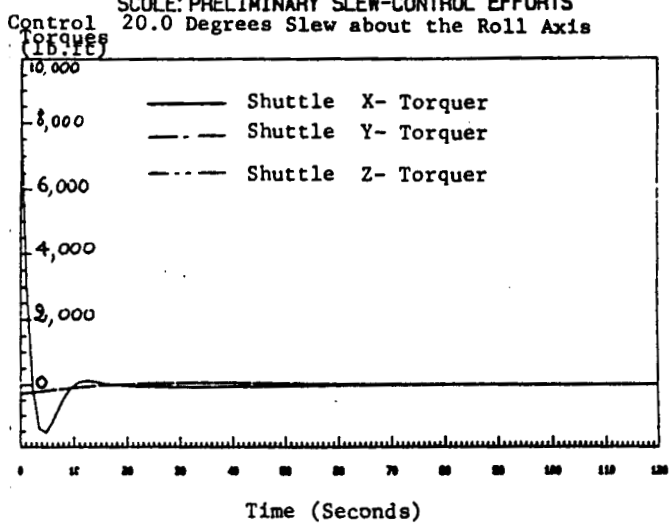

Figure 7:
SCOLE: PRELIMINARY SLEW-CONTROL EFFORTS
20.0 Degrees Slew about the Roll Axis

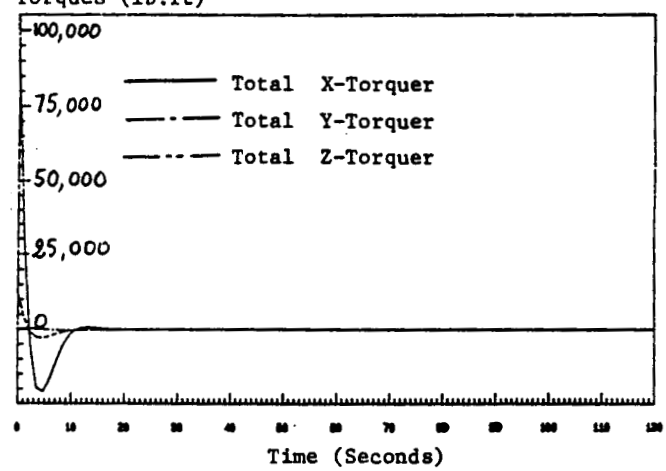

IV. A NUMERICAL APPROACH FOR SOLVING RIGID SPACECRAFT MINIMUM TIME ATTITUDE MANEUVERS

Abstract

The minimum time attitude slewing motion of a rigid spacecraft with its controls provided by bounded torques and forces is considered. Instead of the slewing time, an integral of a quadratic function of the controls is used as the cost function. This enables us to deal with the singular and nonsingular problems in a unified way. The minimum time is determined by sequentially shortening the slewing time. The two-point boundary-value problem is derived by applying the Pontryagin's Maximum Principle to the system and solved by using a quasilinearization algorithm. A set of methods based on the Euler's principal axis rotation are developed to estimate the unknown initial costates and the minimum slewing time as well as to generate the nominal solutions for starting this algorithm.

It is shown that one of the four initial costates associated with the quaternions can be arbitrarily selected without affecting the optimal controls and, thus, simplifying the computation. Several numerical tests are presented to show the applications of these methods.

Introduction

The problems of large-angle attitude maneuvers of a spacecraft have gained much considerations in recent years.[1-9] In these researches, the configurations of the spacecraft considered are: (1) completely rigid, (2) a combination of rigid and flexible parts, or (3) gyrostat-type systems. The performance indices usually include minimum torque integration, power criterion, and frequency-shaped cost functionals, etc. Also some of these investigations utilize feedback control techniques. In this paper, the minimum time attitude slewing control problem of a rigid spacecraft is considered.

In Ref. 2, the problem of the rapid torque-limited slewing of the rigidized SCOLE[1] about a single axis (x-axis) is considered. The control torque about this axis is of a bang-bang type or a bang-pause-bang type. The control laws are developed based on a simplified model of the SCOLE and then used on the practical model (with nonzero products of inertia); hence, this leads to a large error of the attitude after the slewing. Also it seems that no details were given for the controls about the other two axes (y, z).

In the present paper, the optimal control theory (Maximum Principle) is applied to the slewing motion of a general rigid spacecraft (including the rigidized SCOLE, without simplification). The slewing motion need not be restricted to a single-axis slewing. The computational procedure based on a quasilinearization algorithm is developed to solve the resulting two-point boundary-value problem.

Euler Rotation and State Equations

The attitude of a rigid spacecraft can be described by either a quaternion vector $q=[q_0\ q_1\ q_2\ q_3]^T$, which satisfies a constraint equation, $q^Tq=1$, or a direction cosine matrix C,

$$C = \begin{bmatrix} q_0^2+q_1^2-q_2^2-q_3^2 & 2(q_1q_2+q_0q_3) & 2(q_1q_3-q_0q_2) \\ 2(q_1q_2-q_0q_3) & q_0^2+q_2^2-q_3^2-q_1^2 & 2(q_2q_3+q_0q_1) \\ 2(q_1q_3+q_0q_2) & 2(q_2q_3-q_0q_1) & q_0^2+q_3^2-q_1^2-q_2^2 \end{bmatrix} \tag{1}$$

It is known that a single axis rotation of the spacecraft can also be expressed by a quaternion

$$q_0=\cos(\theta/2);\ q_i=e_i\sin(\theta/2),\ i=1,2,3 \tag{2}$$

where θ is the angle of rotation , and e_i are the direction cosines of the rotation axis.

The Euler rotation theorem tells us that an arbitrary orientation of a rigid body can be realized by rotating it about a principal axis (eigenaxis) through a certain angle from its initial position. The desired rotation quaternion, q, between the initial position q(0) and the final orientation $q(t_f)$ can be obtained by the following equation

$$\begin{bmatrix} q_0 \\ q_1 \\ q_2 \\ q_3 \end{bmatrix} = \begin{bmatrix} q_{00} & q_{10} & q_{20} & q_{30} \\ -q_{10} & q_{00} & q_{30} & -q_{20} \\ -q_{20} & -q_{30} & q_{00} & q_{10} \\ -q_{30} & q_{20} & -q_{10} & q_{00} \end{bmatrix} \begin{bmatrix} q_{0f} \\ q_{1f} \\ q_{2f} \\ q_{3f} \end{bmatrix} \tag{3}$$

where the second subscript "$_0$" and "$_f$" represent the initial time and final time, respectively. The angle of rotation and the unit vector, $e=[e_1\ e_2\ e_3]^T$, along this eigenaxis are

$$\theta^*=2\cos^{-1}q_0;\quad e_i=q_i/\sqrt{1-q_0^2},\ i=1,2,3 \tag{4}$$

The equations of motion of a rigid spacecraft are

$$\dot{q}=(1/2)\tilde{\omega}q \tag{5}$$

$$I\dot{\omega}=\tilde{\omega}I\omega+Bu \tag{6}$$

where $\omega=[\omega_1\ \omega_2\ \omega_3]^T$ is the angular velocity vector, B is a 3xn control influence matrix, $u=[u_1\ u_2\ u_3\ \cdots\ u_n]^T$ is the control torque and force vector, and

$$I=\begin{bmatrix} I_{11} & -I_{12} & -I_{13} \\ -I_{12} & I_{22} & -I_{23} \\ -I_{13} & -I_{23} & I_{33} \end{bmatrix}$$

$$\tilde{\omega}=\begin{bmatrix} .0 & \omega_3 & -\omega_2 \\ -\omega_3 & 0 & \omega_1 \\ \omega_2 & -\omega_1 & 0 \end{bmatrix},\qquad \underline{\tilde{\omega}}=\left[\begin{array}{c|c} 0 & -\omega^T \\ \hline \omega & \tilde{\omega} \end{array}\right]$$

Premultiplied by the inverse of I, Eq. (6) can be rewritten as

$$\dot{\omega}=I^{-1}\tilde{\omega}I\omega+I^{-1}Bu \tag{7}$$

The boundary conditions for the states, q and ω, are given as

$$q(0),\ \omega(0);\quad q(t_f),\ \omega(t_f) \tag{8}$$

Optimal Control

Conventionally, the time optimal problem involved here is to seek a solution of Eqs. (5,7) satisfying the boundary conditions (8) and minimizing the slewing time

$$t_f = \int_0^{t_f} (1)dt$$

The control variables must satisfy the constraints

$$|u| \leq u_{imax} = u_{ib}, \quad i=1,2, \ldots, n. \tag{9}$$

The Hamiltonion for this problem can be written as

$$H=1+(1/2)p^T\tilde{\omega}\, q+r^T(I^{-1}\tilde{\omega}\, I\omega+I^{-1}Bu)$$

where p and r are the costate vectors associated with q and ω, respectively. They satisfy the necessary conditions:

$$\dot{p}=-(\partial H/\partial q), \quad \dot{r}=-(\partial H/\partial \omega) \tag{10}$$

By Pontryagin's Maximum Principle, the optimal control minimizing H can be determined by

$$u_i=-u_{ib}\,\mathrm{sgn}(B^TI^{-1}r)_i, \quad i=1,2, \ldots, n. \tag{11}$$

which are of the bang-bang type, except for the singular case in which $(B^TI^{-1}r)_i=0$ over some non-zero time intervals. For the nonsingular bang-bang optimal control problem, a shooting method[10] was tried and failed due to the nonexistence of the inverse of a partial differential matrix.

The singular problem does occur if a special case is considered in the following. When B is a 3x3 unit matrix and I is a diagonal inertia matrix, the control in Eq. (11) is simplified as

$$u_i=-(u_{ib}/I_{ii})\,\mathrm{sgn}(r_i), \quad i=1,2,3 \tag{12}$$

If the state boundary conditions are such that a single principal axis (say, about axis 1) slewing is desired, then a solution satisfying the necessary conditions (10) and equations (5,7) for this problem can be obtained as

$q_0(0)\neq 0,\ q_1(0)\neq 0,\ q_2(0)=q_3(0)=0,$

$\omega_1(0)\neq 0,\ \omega_2(0)=\omega_3(0)=0;$

$q_0\neq 0,\ q_1\neq 0,\ q_2=q_3=0,$

$p_0\neq 0,\ p_1\neq 0,\ p_2=p_3=0,$

$\omega_1\neq 0,\ \omega_2=\omega_3=0;\ r_1=0,\ r_2=r_3=0,$

$u_1=-(u_{1b}/I_{11})\mathrm{sgn}(r_1),\ u_2=u_3=0.$

The solution $r_2=r_3=0$ implies a singular control problem because u_2 and u_3 can not be determined by Eq. (12). The possible existence of a singular solution in the general minimum time problem suggests that a unified method be needed to handle both singular and nonsingular cases.

In some papers[3,8], the integral of the sum of the squares of the torque components has been successfully used as a cost function, where there is no constraint on the control and the minimum time is not required. However, if some constraints on the control are added to this problem and the total slewing time is shortened sequentially, this problem may approach the minimum time control problem. These considerations motivate a successive approximation approach to solve the minimum time control problem. In this approach, an integral of a quadratic function of the controls is formally used as a cost function, i.e.,

$$J=(1/2)\int_0^{t_f} u^T R u\,dt \qquad (13)$$

where R is a proper weighting matrix. It has been shown that[3,8], for the case of rest-to-rest slewing with only 3 control inputs involved and with a longer slewing time used, the controls are approximately linear functions of time and do not reach their saturation levels. Therefore, when t_f is shortened, some of the controls can be expected to reach their bounds and contribute more effort to the slewing. By the successive shortening of t_f, a particular value, t_f^*, called the minimum time, can be obtained, during which either some (singular case) or all (nonsingular case) of the controls are of the bang-bang type.

Apparently, in the approach described above, it is unnecessary to determine in advance whether the problem is singular or not and there is no need to determine the switching points as required in some other methods[10].

Necessary Conditions

The Hamiltonion for the system (5,7,13) is then

$$H=(1/2)u^TRu+p^T\tilde{\omega}q+r^T(I^{-1}\tilde{\omega}I\omega+I^{-1}Bu) \qquad (14)$$

where the costates, as before, satisfy the following necessary conditions for minimizing J,

$$\dot{p}=-(\partial H/\partial q), \text{ or } \dot{p}=(1/2)\tilde{\omega}p \qquad (15)$$

$$\dot{r}=-(\partial H/\partial \omega), \text{ or } \dot{r}=g(\omega,r)+(1/2)[q]p \qquad (16)$$

where $g(\omega, r)$ is a 3x1 vector function of ω and r, and its detailed form can be found in Appendix A; [q] is a 3x4 matrix

$$[q]=\begin{bmatrix} q_1 & -q_0 & -q_0 & q_2 \\ q_2 & q_3 & -q_0 & -q_1 \\ q_3 & -q_2 & q_1 & -q_0 \end{bmatrix}$$

The initial values of p and r are unknowns.

The weighting matrix R in Eq. (13) is chosen as

$$R=B^TB \tag{17}$$

which is generally an nxn semi-positive-definite matrix, because the rank of the 3xn matrix, B, is assumed to be 3. Weighting matrices other than that given by Eq. (17) may also be possible candidates.

From the necessary conditions $(\partial H/\partial u)=0$, we have

$$Ru+B^TI^{-1}r=0$$

or

$$B^TBu=-B^TI^{-1}r \tag{18}$$

Premultiplying both sides of Eq. (18) by $(BB^T)^{-1}B$, one obtains,

$$Bu=-I^{-1}r$$

By using the pseudo-inverse of the matrix B, B^+, one can get u,

$$u=-B^+I^{-1}r=-B^T(BB^T)^{-1}(I^{-1}r) \tag{19}$$

The control laws are then[11]

$$u_i=-u_{ib}\,\mathrm{sgn}(B^+I^{-1}r)_i, \text{ if } |(B^+I^{-1}r)_i| \geq u_{ib}; \tag{20a}$$

or

$$u_i=-(B^+I^{-1}r)_i, \text{ if } |(B^+I^{-1}r)_i| < u_{ib} \tag{20b}$$

$$i=1,2, \ldots, n.$$

note that when B is a 3x3 nonsingular matrix, $B^+=B^{-1}$.

A Linear Relation between q and p

Before starting to solve the two-point boundary-value problem, it is useful to consider a relationship between q and p. It is already pointed out in Ref. 9 that

$$p = \rho q$$

where ρ is an arbitrary constant. However, one can find out that there does exist a linear relation between p and q in this problem,

$$p(t) = Dq(t) \tag{21}$$

where D is a 4x4 constant matrix. To determine the constant elements of D, Eq. (21) is substituted into the differential equation for p in Eq. (15), with the result,

$$D\dot{q} = (1/2)\tilde{\omega} Dq \tag{22}$$

The $\dot{q}$ in Eq. (22) is then replaced by Eq. (5),

$$D(1/2)\tilde{\omega} q = (1/2)\tilde{\omega} Dq \tag{23}$$

Since Eq. (23) is valid for arbitrary q, one has

$$D\tilde{\omega} = \tilde{\omega} D$$

This relation is true for arbitrary values of ω only when D has the following form

$$D = \begin{bmatrix} d_0 & -d_1 & -d_2 & -d_3 \\ d_1 & d_0 & -d_3 & d_2 \\ d_2 & d_3 & d_0 & -d_1 \\ d_3 & -d_2 & d_1 & d_0 \end{bmatrix} \tag{24}$$

and these constants, d_0, d_1, d_2, d_3, can be determined by setting t=0 in Eq. (21). With the use of Eq. (24), the relation (21) can be rewritten as

$$\begin{bmatrix} p_0 \\ p_1 \\ p_2 \\ p_3 \end{bmatrix} = \begin{bmatrix} q_0 & -q_1 & -q_2 & -q_3 \\ q_1 & q_0 & q_3 & -q_2 \\ q_2 & -q_3 & q_0 & q_1 \\ q_3 & q_2 & -q_1 & q_0 \end{bmatrix} \begin{bmatrix} d_0 \\ d_1 \\ d_2 \\ d_3 \end{bmatrix} \tag{25}$$

After substituting Eq. (25) into Eq. (16), there results

$$\dot{r}=g(\omega, r)-(1/2)Cd \tag{26}$$

where $d=[d_1\ d_2\ d_3]^T$, C is just the attitude matrix, Eq. (1). It can be seen from Eq. (26) that r is independent of d_0. It is also true that u is independent of d_0 because u depends only on r in Eqs. (20). This means that the arbitrary selection of d_0 yields the same extremum control, u. It is noted that a special choice of d_0 can lead to the equivalent conditions considered in Refs. 3 and 9. With the use of Eq. (25), one can get

$$d_0^2+d_1^2+d_2^2+d_3^2=p^T(0)P(0) \tag{27}$$

Since the choice of d_0 is independent of the choice of d_1, d_2, and d_3, a minimum value of the left side (hence the right side) of Eq. (27) is reached when $d_0=0$. This is the solution considered in Ref. 3. Also from Eq. (25) one can get

$$d_0=p^T(0)q(0)$$

When $d_0=0$, this equation gives a constraint on p(0). It is suggested in Ref. 9 that this constraint be used in the numerical iterations. But the choice of d_0 other than zero is a more general result for this problem. It is not necessary to keep $d_0=0$ in each step of the computation. It is enough to keep one element of p(0) unchanged which is easier to use than the approach suggested in Ref. 9, especially when $q(0)\neq[1\ 0\ 0\ 0]^T$.

Initial Values of Costates and the Slewing Time

Since the Euler rotation brings the attitude of the spacecraft from an initial quaternion to a final required quaternion through a simple rotation, it may take less time and consume less energy; it is reasonable to choose this rotation as a candidate for the starting solution of the iteration and hope that the optimal slewing is near the Euler rotation. This rotation will be called the "expected rotation", which is determined only by $q(0)$ and $q(t_f)$.

The angular velocity and its derivatives for the Euler rotation can be expressed as

$$\bar{\omega}=\dot{\theta}e, \quad \dot{\bar{\omega}}=\ddot{\theta}e, \quad \ddot{\bar{\omega}}=\dddot{\theta}e \tag{28}$$

where $\theta(t)$ is the rotation angle and $e=[e_1\ e_2\ e_3]^T$ is a unit vector along the the rotation axis (eigenaxis) which is determined by Eq. (4). Considering the analytical solution about a single principal axis maneuver in Ref. 3, θ can be defined the same way about e,

$$\theta(t)=\theta(0)+\dot{\theta}(0)t+(1/2)\ddot{\theta}(0)t^2+(1/6)\dddot{\theta}(0)t^3 \tag{29}$$

where $\theta(0)$, $\dot{\theta}(0)$, $\ddot{\theta}(0)$, and $\dddot{\theta}(0)$ can be determined from the boundary conditions of $\theta(t)$ and $\dot{\theta}(t)$ at $t=0$, and $t=t_f$.

Without loss of generality, one can choose

$$\theta(0)=0, \quad \theta(t_f)=\theta^* \tag{30a}$$

where θ^* is given in Eq. (4), and

$$\dot{\theta}(0)=\dot{\theta}_0, \quad \dot{\theta}(t_f)=\dot{\theta}_f \tag{30b}$$

The value of $\dot{\theta}_0$ in Eq. (30b) needs to be determined from a given initial angular velocity vector, $\omega(0)$. Generally, this vector will not coincide with $\bar{\omega}(0)$, the angular velocity of the Euler rotation at t=0, defined in Eq. (28), therefore, a difference vector, ε, between them exists,

$$\varepsilon = \dot{\theta}_0 e - \omega(0)$$

Since only an approximate starting solution of the quasilinearization method is needed, it is enough to choose a $\dot{\theta}_0$ which minimizes $\varepsilon^T\varepsilon$. By differentiating $\varepsilon^T\varepsilon$ with respect to $\dot{\theta}_0$ and noting that $e^Te=1$, one can get

$$\dot{\theta}_0 = e^T \omega(0) \tag{31}$$

A similar derivation for $\dot{\theta}_f$ can be obtained.

For the special case of $\dot{\theta}_f=0$, the substitution of Eqs. (30) into Eq. (29) will result in

$$\ddot{\theta}(0) = (6\theta^*/t_f^2) - (4\dot{\theta}_0/t_f) \tag{32a}$$

$$\dddot{\theta}(0) = -(12\theta^*/t_f^3) + (6\dot{\theta}_0/t_f^2) \tag{32b}$$

To approximately determine the initial values of p and r, Eqs. (7) and (26) are needed. By substituting u in Eq. (19) into Eq. (7) and solving for r, one can get

$$r = I\tilde{\omega}I\omega - I^2\dot{\omega} \tag{33}$$

$$\dot{r} = (d/dt)(I\tilde{\omega}I\omega) - I^2\ddot{\omega} \tag{34}$$

At the same time, Eq. (26) can be rewritten as

$$d = 2C^T[g(\omega, r) - \dot{r}] \tag{35}$$

Replacing ω in Eqs. (33-35) by the relations (28-32) at t=0, one can get the approximate values of r(0) and d. p(0) can be determined by letting one of its elements equal a constant (say $p_0(0)$=constant, if $q(0)=[1\ 0\ 0\ 0]^T$) and by using Eq. (25) to solve for d_0 and other elements of p(0).

The starting solution needed in the quasilinearization algorithm may be obtained by integrating the differential equations (5,7,15-16,20) using the initial conditions p(0) and r(0) obtained above, as well as q(0) and $\omega(0)$.

Initial Value of t_f

Generally, to obtain the minimum time, one can always choose a longer slewing time, t_f, at the beginning of the algorithm, and shorten it sequentially thereafter. But this may take more time, especially when how far the initial choice is from the real minimum time is not known. Therefore, a good initial value of t_f being close to and larger than the minimum value is desired. For simplicity, only an estimation procedure of t_f for the case in which B is a 3x3 unit matrix is discussed here. Suppose the slewing motion is an Euler rotation about a vector, e, through an angle, $\theta(t)$. By using the relations for ω in Eq. (28) into Eq. (6), one can get

$$Ie\ddot{\theta}=\dot{\theta}^2\tilde{e}Ie+u$$

which can be expressed as the following 3 similar equations

$$a_i\ddot{\theta}=b_i\dot{\theta}^2+c_i\tau_i, \quad i=1,2,3 \tag{36}$$

where a_i and b_i are constants, $c_i=u_{ib}$, and τ_i is the normalized

control about the ith body axis and

$$|\tau_i| \leq 1, \quad i=1,2,3$$

The 3 equations of Eq.(36) must be simultaneously valid for the same $\theta(t)$. Each of them with the boundary conditions, (30), can be considered as a minimum time control problem and solved analytically to obtained a minimum time (Appendix B). Since each of the minimum times for the associated equation means a lower bound of time during which the equation is solvable (no matter whether this equation is treated as a minimum time control problem or not), the largest one of these minimum times should be chosen as the initial value of t_f used in the computation.

A computation procedure has been developed which contains a series of cycles. The slewing time is chosen at the beginning of each cycle and fixed throughout the cycle. During each cycle, a quasilinearization algorithm called the method of particular solutions[12] is used to solve the linearized state and costate equations. If this algorithm converges, a check is then made as to whether some (singular case) or all (nonsingular case) of the controls are of the bang-bang type. If yes, this slewing time is designated the minimum time. If not, the assumed t_f should be shortened and the next cycle begins.

The numerical experience of using this procedure tells us that, for each cycle, the slewing time can not be made less than a certain value; in particular, it can not be made less than the real minimum time. Otherwise, the algorithm in each cycle will not converge. The closer the t_f is to the real minimum time, the less shortening is required for the t_f assumed in the previous cycle.

Numerical Results

The methods described in the previous sections are applied to the SCOLE slewing motion. Fig. 1 shows the SCOLE configuration. It is composed of a Space Shuttle and a large reflecting antenna. The antenna is attached to the Shuttle by a flexible beam. Since only the motion of the rigid SCOLE is considered in this paper, the flexibility of the beam is ignored. The X, Y, and Z axes are the Shuttle axes corresponding to the roll, pitch, and yaw axes, respectively. The controls considered in this paper include three moments ($u_x=u_1, u_y=u_2, u_z=u_3$) about the X, Y, and Z axes and two forces ($f_x=u_4$, $f_y=u_5$) applied at the center of the reflector in the X and Y directions. The inertia parameters of the SCOLE and the saturation levels of the controls are[1]:

$I_{11}=1132508$, $I_{22}=7007447$, $I_{33}=7113962$,

$I_{12}=-7555$, $I_{23}=115202$, $I_{13}=52293$ slug-ft^2;

$u_{ib}=10000$ ft-lb, i=1,2,3;

$u_{ib}=800$ lb., i=4,5

The associated control influence matrix, B, in Eq. (6) is

$$B=\begin{bmatrix} 1 & 0 & 0 & 0 & 130 \\ 0 & 1 & 0 & -130 & 0 \\ 0 & 0 & 1 & 32.5 & 18.75 \end{bmatrix}$$

Some numerical results are presented in the following.

(a) The singular case discussed in the previous sections for the SCOLE configuration without offset and for a symmetrical Shuttle $I_{12}=I_{23}=0$. For this case only the three Shuttle control torquers are used. The boundary conditions of the attitude are

such that the "expected rotation" is a single principal axis rotation. The computations show that when the slewing time approaches the minimum time, the control about the the slewing axis approaches the bang-bang type. The other two controls remain zero and there is no indication that they are going to make contributions to speed up the slewing. This result may imply that the singular solution is the time optimal solution for this case; otherwise additional control effort should participate in the slewing and a smaller slewing time should be obtained by using this algorithm.

(b) The example of Ref. 3 is computed to test the method of determination of the initial costates. The results show that the guessed initial costates are very close to their converged values. To obtain the converged values (to seven digits), only 5 iterations are needed in this computation.

(c) The non-diagonal inertia matrix of the SCOLE and only 3 controls (u_1, u_2, u_3) are used in this case. The expected rotation is a 20 degree, rest-to-rest rotation about one of the three spacecraft axes. Only the results for the "X-axis slewing" are given here because the results for the "Y-axis and Z-axis slewings" are similar. Figs. 2 show the time histories of the controls and attitude angles (1-2-3 Euler angles) for this maneuver. Due to the non-zero offset of the inertia distribution of the SCOLE configuration, the controls, u_y and u_z, are no longer zero as they were in the singular case (a), but now are of the bang-bang type. The initial estimation of the minimum slewing time, t_f, obtained using the method discussed in the

previous section , is $t_f^{(0)}$=12.5749 sec, which is very close to the minimum time, t_f^*=12.563034 sec, obtained in our computation.

Fig. 3 shows the control torques for the "X-axis slewing" described in case (a) but for a slewing time, t_f=15.37 sec, which is 2.8 seconds more than the minimum time, t_f^*. The controls are almost linear functions of time. u_1 is less than the saturation level; u_2 and u_3 are near zero. By comparing Fig. 3 with Fig. 2a, one can see that much more control effort (approximate 50%) is saved by using a little longer slewing time. Another feature of using a longer slewing time in the computation is that it needs fewer iterations for convergence than by using a shorter slewing time. These properties imply that, in the practical application of this problem, it is not necessary to seek exactly the minimum time, t_f^*, and the associated extremum controls. It may be enough to know the approximate values of t_f^* and the controls.

(d) Following case (c), two additional controls, u_4 and u_5, corresponding to the thrusters on the reflector are used. Figs. 4 show the controls and attitude angles for the "X-axis slewing". The minimum time, t_f^*=3.9805382 sec, is greatly shortened as compared with case (c). Figs. 5 show the controls and attitude angles for the "Z-axis slewing". The minimum time is t_f^*=15.1441 sec. Unlike the case for the X-axis slewing, the attitude angle θ_x experiences a larger amplitude, though the expected rotation is about the Z-axis. This phenomenon is due to

the unsymmetric distributions of inertia about the X and Y axes. The closer the slewing is to the minimum time, the larger the amplitude of the θ_X.

(e) A general case is considered. Suppose the SCOLE is in an Earth orbit and the line of sight is to be directed toward the center of the Earth. The orbit coordinate system (x,y,z) is shown in Fig. 6. The initial attitude of the spacecraft is assumed as follows: the Y axis coincides with the orbital y axis, and the angular difference between the X and x (or Z and z) axes is α=7.897224212 deg . The initial quaternion is, then, $q(0)=[\cos(\alpha/2) \quad 0 \quad \sin(\alpha/2) \quad 0]^T$. According to Ref. 1, the unit vector along the line of sight in the rigid SCOLE coordinate system is

$$\hat{R}_{LOS}=[.1112447 \quad -.2410302 \quad .9641209]^T$$

The direction cosines of the orbital z axis in the SCOLE system at the initial time are $\hat{z}_{/B}=[\sin\alpha \quad 0 \quad \cos\alpha]^T$. The angle between $\hat{R}_{LOS}$ and $\hat{z}_{/B}$ at the initial time is $\theta_{LOS}(0)= \hat{R}_{LOS}\cdot\hat{z}_{/B}$=20 deg . The eigenaxis of the expected rotation in the SCOLE system is determined by

$$e=(\hat{R}_{LOS}x\hat{z}_{/B})/|\hat{R}_{LOS}x\hat{z}_{/B}|$$

The final required attitude quaternion can be obtained by using Eqs. (3-4).

The guessed minimum time for the case where only 3 controls are involved in this maneuver is t_f=26.3487 sec . This value is very close to the converged value, t_f^*=25.003175 sec . It would be interesting if this estimation is compared with the result by solving the following classical minimum time control problem,

$$I\ddot{\theta}=u, \qquad |u| \leq u_{max}$$

where I is the moment of inertia about the principal line and u is the torque about that line, θ is the angle of rotation. For the present case, the result obtained from the second method is t_f=19.58 sec . A possible explanation for the large difference here is that the classical problem greatly simplifies the inherent three dimensional nonlinear dynamics associated with the general SCOLE configuration.

Figs. 7 show the controls and attitude angles for case (e) where u_4 and u_5 are also used. The minimum slewing time is obtained as t_f^*=8.691397 sec . The θ_{LOS} in Fig. 7b is the angle between the line of sight and the line of the target direction (from the spacecraft to the center of the Earth).

Conclusions

A useful numerical solution procedure for the minimum time attitude maneuver control problem of a rigid spacecraft has been developed and successfully applied to some practical examples. It can handle both the singular and nonsingular cases. It is shown through examples that the estimation methods used here for the initial costates and the minimum slewing time are quite useful. The control profiles obtained in this paper may be useful for further research.

References

[1]Taylor, L.W. and Balakrishnan, A.V., "A Mathematical Problem and a Spacecraft Control Laboratory Experiment (SCOLE) used to Evaluate Control Laws for Flexible Spacecraft ... NASA/IEEE Design Challenge", Jan., 1984. (Proceedings of the 4th VPI&SU Symposium on Dynamics and Control of Large Structures, Blacksburg, VA, June 1983)

[2]Lin, J.G., "Rapid Torque-Limited Line-of-sight Pointing of SCOLE (Spacecraft Control Laboratory Experiment) Configuration," AIAA/AAS Astrodynamics Conference, Williamsburg, VA, Aug. 1986, AIAA paper 86-1991.

[3]Junkins, J.L. and Turner, J.D., "Optimal Continuous Torque Attitude Maneuvers," Journal of Guidance and Control, Vol. 3, No. 3, May-June 1980, pp. 210-217.

[4]Skaar, S.B. and Kraige, L.G., "Large-Angle Spacecraft Attitude Maneuvers Using an Optimal Reaction Wheel Power Criterion," The Journal of the Astronautical Sciences, Vol. 32, No. 1, Jan.-March 1984, pp. 47-61.

[5]Chen, J. and Kane, T.R., "Slewing Maneuvers of Gyrostat Spacecraft," The Journal of the Astronautical Sciences, Vol. 28, No. 3, July-Sept. 1980, pp. 267-281.

[6]Turner, J.D. and Junkins, J.L., "Optimal Large-Angle Single-Axis Rotational Maneuvers of Flexible Spacecraft," Journal of Guidance and Control, Vol. 3, No. 6, Nov.-Dec. 1980, pp. 578-585.

[7]Chun, H.M. and Turner, J.D., "Frequency-Shaped Large-Angle Maneuvers," AIAA 25th Aerospace Sciences Meeting, Jan. 12-15, 1987, Reno, Nevada, AIAA paper 87-0174.

[8]Bainum, P.M. and Li, F., "Optimal Torque Control SCOLE Slewing Maneuvers," 3rd Annual SCOLE Workshop, Nov. 17, 1986, NASA Langley Research Center, Hampton, Virginia.

[9]Vadali, S.R., Kraige, L.G. and Junkins, J.L., "New Results on the Optimal Spacecraft Attitude Maneuver Problem," Journal of Guidance and Control, Vol. 7, No. 3, May-June 1984, pp. 378-380.

[10]Lastman, G.J., "A Shooting Method for Solving Two-Point Boundary-Value Problems Arising from Non-Singular Bang-Bang Optimal Control Problems," Int. Journal of Control, Vol. 27, No. 4, 1978, pp. 513-524.

[11]Yeo, B.P., Waldron, K.J. and Goh, B.S., "Optimal Initial Choice of Multipliers in the Quasilinearization Method for Optimal Control Problems with Bounded Controls," Int. Journal of Control, Vol. 20, No. 1, 1974, pp. 17-33.

[12]Miele, A. and Iyer, R.R., "General Technique for Solving Nonlinear Two-Point Boundary-Value Problems Via the Method of Particular Solutions," Journal of Optimizatiom Theory and Applications, Vol. 5, No. 5, 1970, pp. 382-399.

Appendix A The Term g(ω, r) in Eq. (16)

The term $I^{-1}\tilde{\omega}I\omega$ in Eq. (7) can be expressed as

$$I^{-1}\tilde{\omega}I\omega=[F:G]\,\bar{\bar{\omega}}$$

and

$$\bar{\bar{\omega}}=[\,\omega_1^2 \quad \omega_2^2 \quad \omega_3^2 \quad \omega_2\omega_3 \quad \omega_3\omega_1 \quad \omega_1\omega_2]^T$$

where F and G are 3x3 matrices whose elements are constants associated with the inertia parameters of the spacecraft. Then the term $r^TI^{-1}\tilde{\omega}I\omega$ of the Hamiltonion, H, in Eq. (14) has the form

$$h=r^TI^{-1}\tilde{\omega}I\omega=[f_1\ f_2\ f_3\ f_4\ f_5\ f_6]^T\,\bar{\bar{\omega}}$$

where f_i are

$$[f_1\ f_2\ f_3]^T=F^Tr, \quad [f_4\ f_5\ f_6]^T=G^Tr$$

The term g(ω, r) in Eq. (16) can be obtained by

$$g(\omega, r)=-(\partial h/\partial\omega)=-\begin{bmatrix}2f_1 & f_6 & f_5\\ f_6 & 2f_2 & f_4\\ f_5 & f_4 & 2f_3\end{bmatrix}\begin{bmatrix}\omega_1\\ \omega_2\\ \omega_3\end{bmatrix}$$

Appendix B Solution of Eq. (36)

Eq. (36) can be rewritten as

$$a_i\ddot{\theta}=b_i\dot{\theta}^2+c_i\tau_i \tag{36}$$

For simplicity, only the solutions for the following boundary conditions are considered here

$$\theta(0)=0,\ \dot{\theta}(0)=0;\ \theta(t_f)=\theta^*,\ \dot{\theta}(t_f)=0 \tag{B-1}$$

Suppose $a_i\neq0$, $b_i\neq0$ and let $b=b_i/a_i$, $c=c_i/a_i$ (suppose $c>0$), one can rewrite Eq. (36) as

$$\ddot{\theta}=b\dot{\theta}^2+c\tau \qquad \text{(B-2)}$$

Since the control for this problem is of a bang-bang type with only one switching point, by integrating Eq. (B-2) and using Eq. (B-1), one can get

$$\dot{\theta}=[c(e^{2b\theta}-1)/b]^{1/2}, \text{ for } \tau=1; \qquad \text{(B-3)}$$

$$\dot{\theta}=[c(1-e^{2b(\theta-\theta^*)})/b]^{1/2}, \text{ for } \tau=-1 \qquad \text{(B-4)}$$

By equating Eqs. (B-3) and (B-4), one can get $\theta=\theta_s$ and $\dot{\theta}=\dot{\theta}_s$ at the switching point, $t=t_s$,

$$\theta_s=(1/2b)\ln[2/(1+e^{-2b\theta^*})]$$

$$\dot{\theta}_s=[c(e^{2b\theta_s}-1)/b]^{1/2}$$

Finally, by integrating Eqs. (B-3,4) and using Eq. (B-1), one can get

$$t_s=\cosh^{-1}(e^{-b\theta_s})/\sqrt{-bc}, \quad b<0;$$

or

$$t_s=[(\pi/2)-\sin^{-1}(e^{-b\theta_s})]/\sqrt{bc}, \quad b>0$$

and

$$t_f=t_s+[(\pi/2)-\sin^{-1}(e^{b(\theta^*-\theta_s)})]/\sqrt{-bc}, \quad b<0;$$

or

$$t_f=t_s+\cosh^{-1}(e^{b(\theta^*-\theta_s)})/\sqrt{bc}, \quad b>0$$

For the case $\dot{\theta}(0)\neq 0$, similar solutions can be obtained.

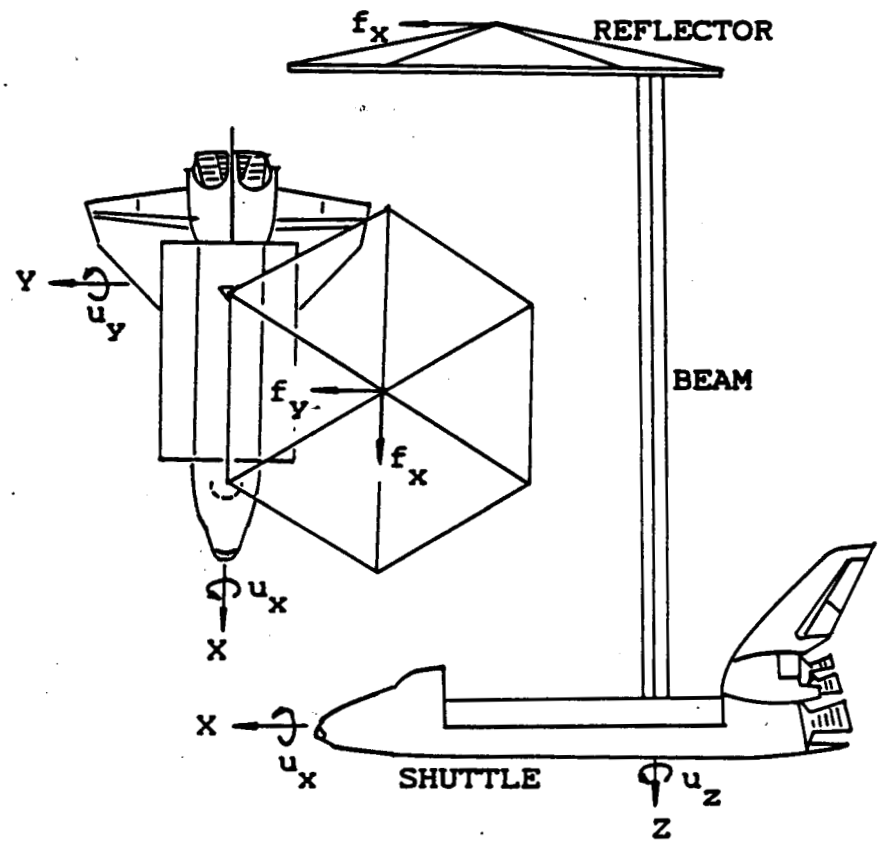

Fig. 1 Spacecraft Control Laboratory Experiment configuration (SCOLE)

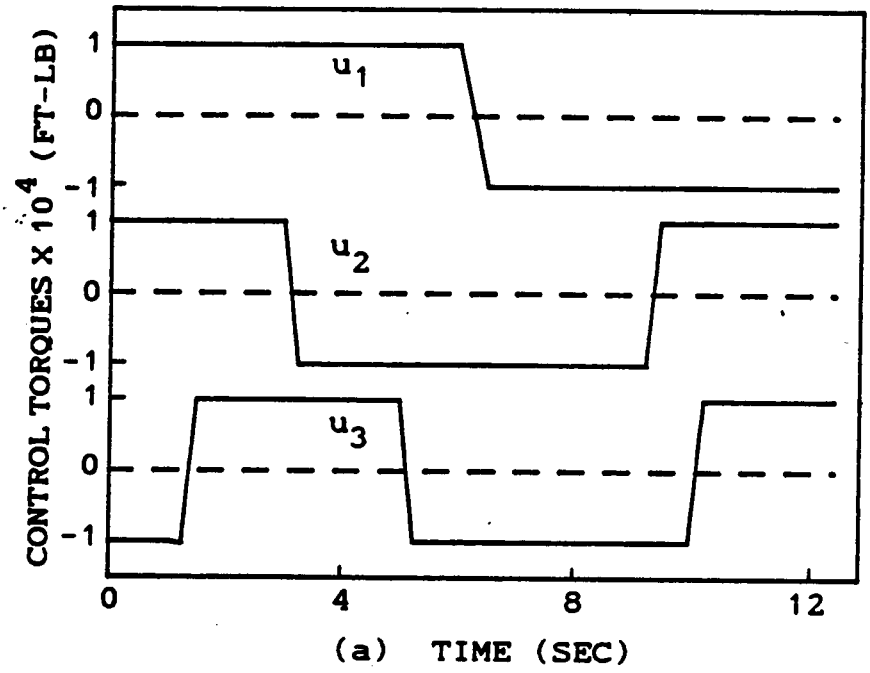

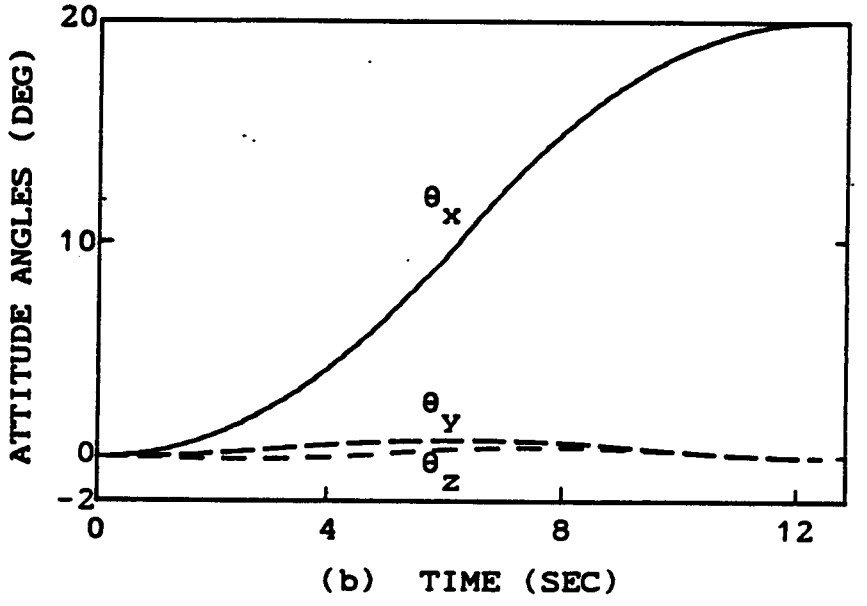

Fig. 2 X-axis slewing, t_f=12.563034 (s)

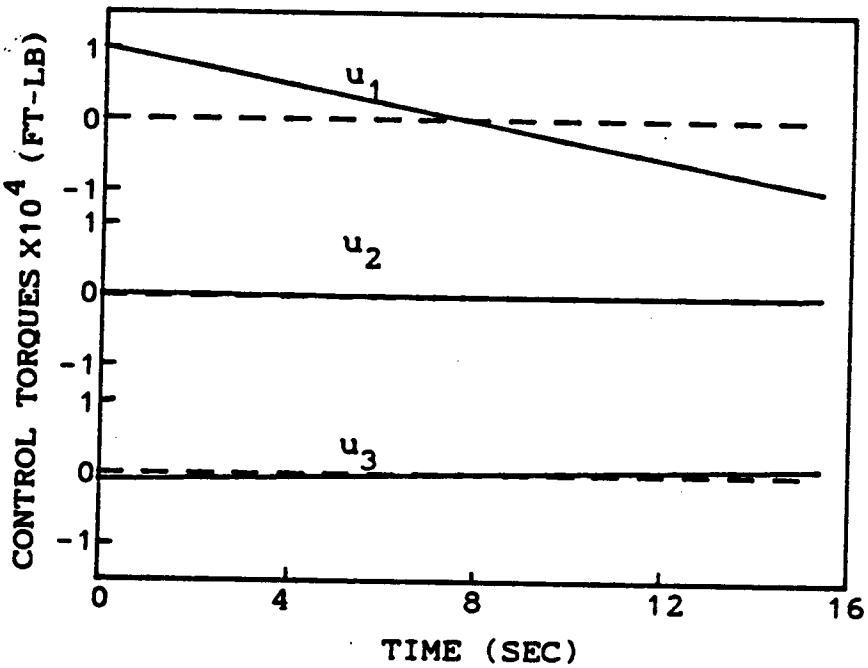

Fig. 3 X-axis slewing, t_f=15.37 (s)

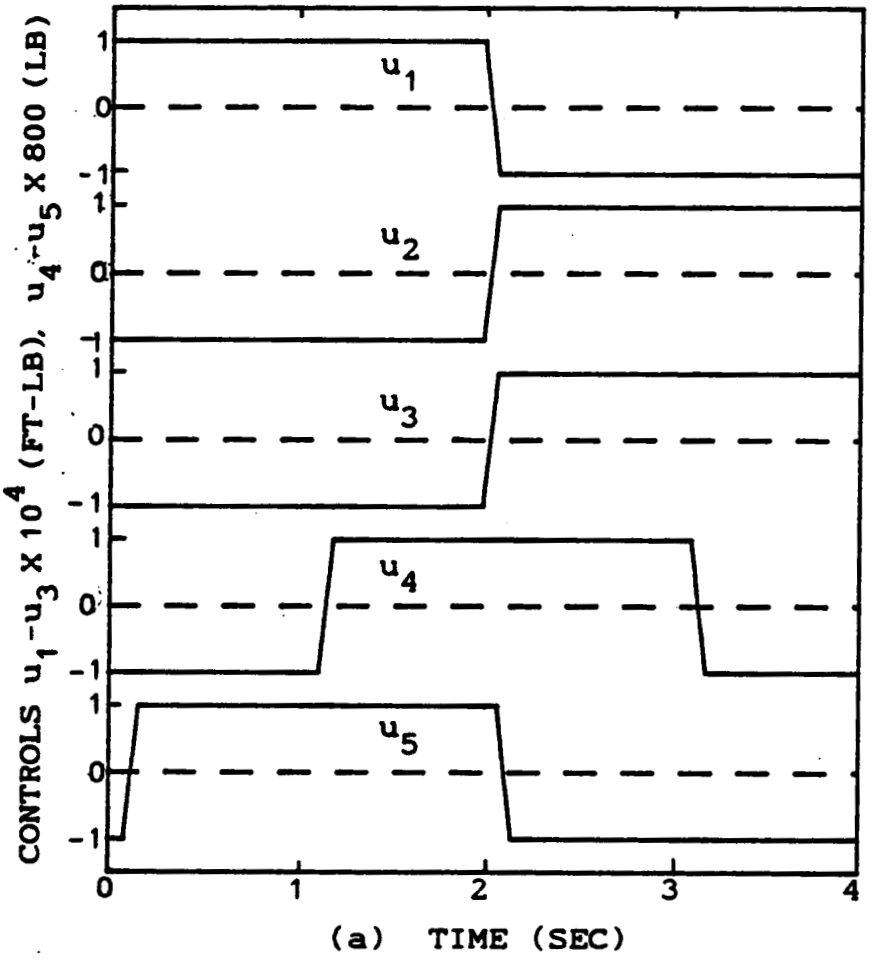

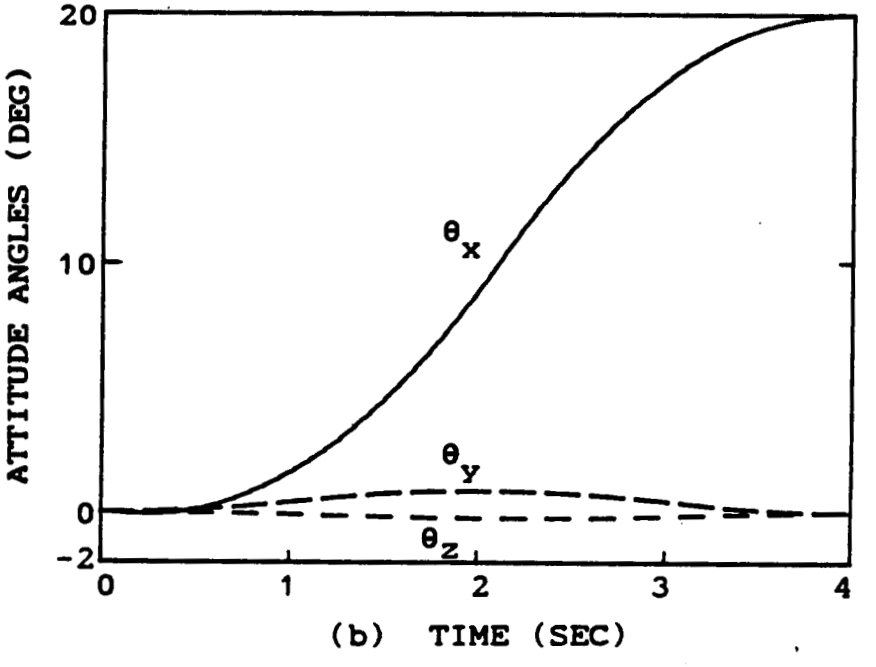

Fig. 4 X-axis slewing, t_f=3.9805382 (s)

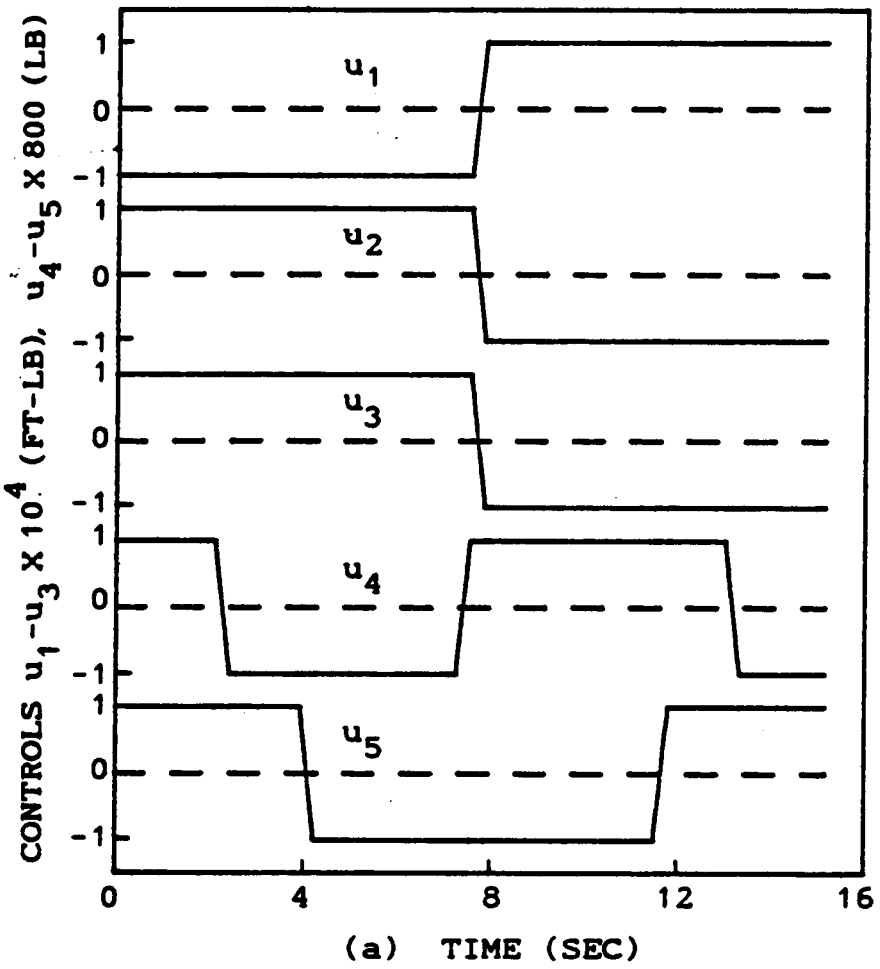

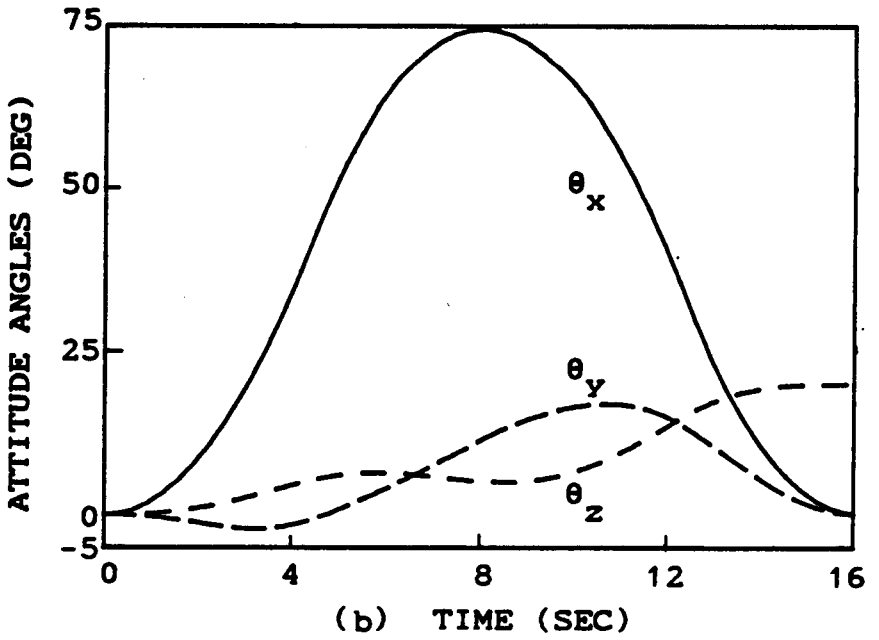

Fig. 5 Z-axis slewing, t_f=15.1441 (s)

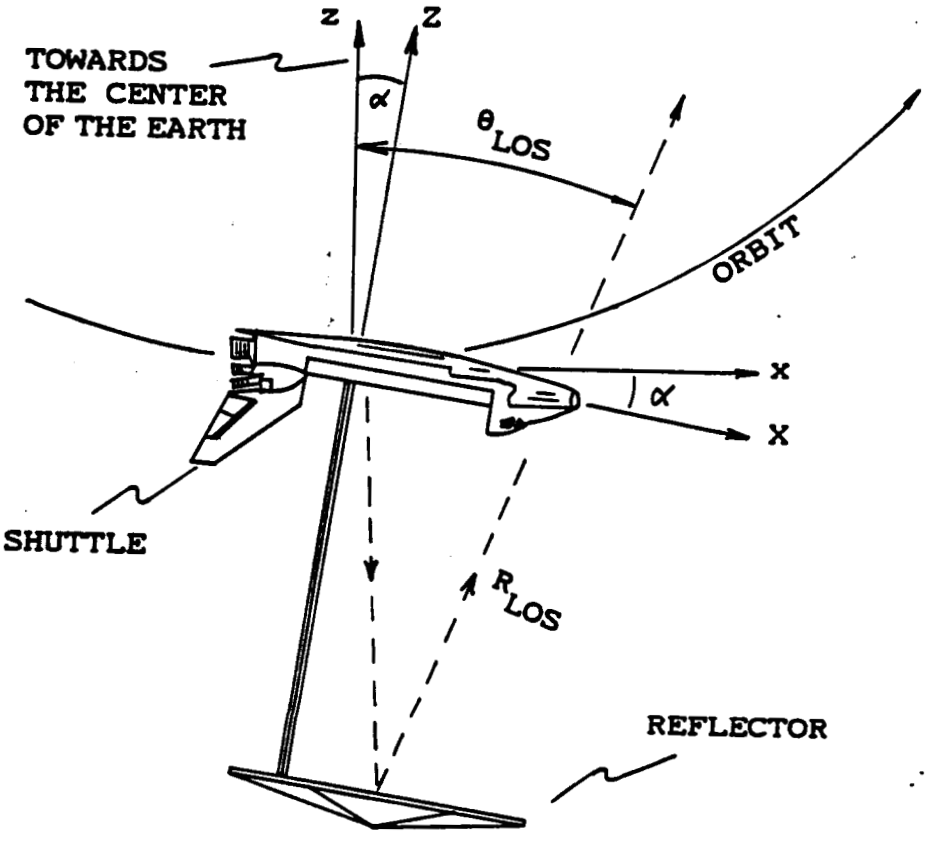

Fig. 6 Attitude of the SCOLE showing antenna line of sight

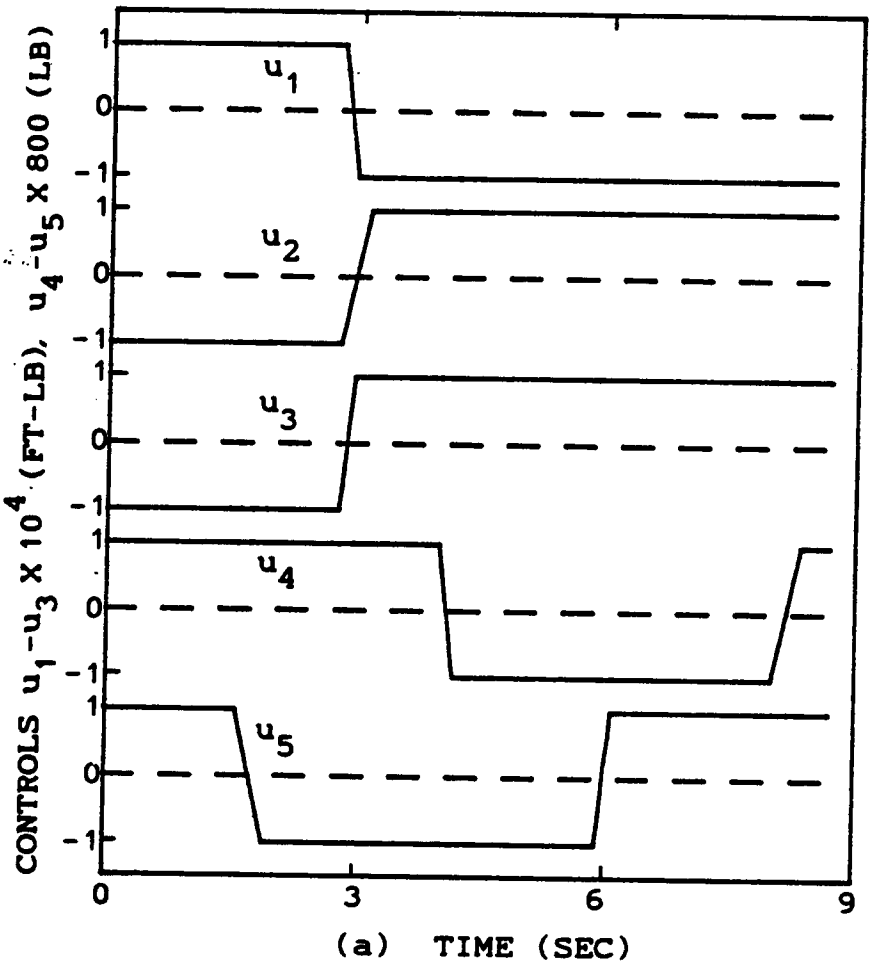

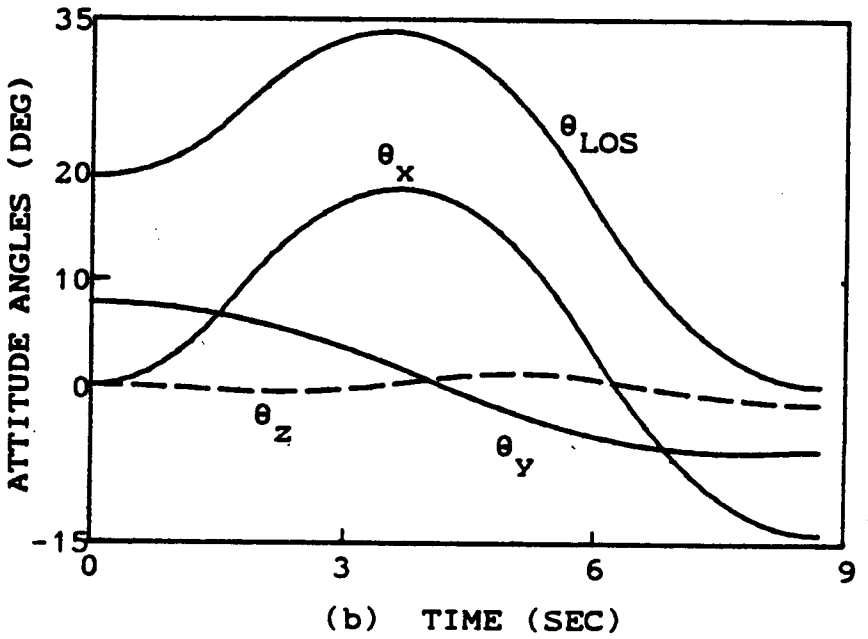

Fig. 7 SCOLE-example LOS slewing, t_f=8.691397 (s)

V. ASPECTS OF COMPUTATIONAL REQUIREMENTS FOR CONTROLLER IMPLEMENTATION

V.I Discretization of Continuous Controllers:

The full state variable feedback of the form

$$U = KX \tag{1}$$

is usually proposed to control a linear plant given by

$$\dot{X} = AX + BU \tag{2}$$

using techniques such as pole placement[1], Linear Quadratic Gaussian/Loop transfer recovery (LQG/LTR)[2], H_∞ techniques[3], etc. The implementation of the controller given in (1) and the generally needed state estimator are implemented using a microprocessor and thus the stability of the discretized control law as a function of the discretization step size is to be evaluated.

To this end, the system dynamics and the control law as given by (2) and (1) are discretized using Euler's scheme as:

$$X(i+1) = (I + \Delta(A+BK))\, X(i) \tag{3}$$

with

$$U(i) = KX(i) \tag{4}$$

Balas[4] has shown, using Lyapunov's stability criteria, that the stable continuous control law given by (2) is stable in the discrete time domain provided

$$\Delta < \frac{\lambda_{min}(Q)}{\lambda_{max}\,(A_c^T P A_c)} \tag{5}$$

where

Q = any positive definite matrix

P is the solution of the Lyapunov's equation

$$PA_c + A_c^T P + Q = 0$$

λ_{min} ( ) , λ_{max} ( ) are the minimum and maximum eigenvalues of the matrices in the parenthesis

$$A_c = A + BK$$

The disadvantage of the criteria (5) is its dependence on an arbitrary Q matrix and thus the absolute maximum value of Δ cannot be obtained.

An improved stability criteria can be developed using the modal transformation on the closed loop system

$$\dot{X} = (A + BK)X \tag{6}$$

or $$\dot{X} = A_c X \tag{7}$$

as $$X = T\, q \tag{8}$$

$$\dot{q} = \Lambda\, q \tag{9}$$

where $\Lambda = \text{diag}\ (\lambda_1, \lambda_2, \ldots, \lambda_n)$

λ_i = ith eigenvalue of the matrix A_c and the eigenvalues are assumed to be distinct.

The same transformation is applied to equation (3) as[5]

$$q(i+1) = T^{-1}(I + \Delta A_c)T\, q\ (i) \tag{10}$$

or $$q_\ell(i+1) = (1 + \Delta\lambda_\ell)\ q_\ell(i) \tag{11}$$

$$\ell = 1,2,\ldots, n.$$

The ℓth difference equation is stable in the discrete time domain provided

$$|1 + \Delta\lambda_\ell| < 1 \tag{12}$$

or $$(1 + \Delta\sigma_\ell)^2 + (\Delta\omega_\ell)^2 < 1 \tag{13}$$

where

$$\lambda_\ell = \sigma_\ell + j\,\omega_\ell \tag{14}$$

i.e.

$$\Delta(2\sigma_\ell + \Delta(\sigma_\ell^2 + \omega_\ell^2)) < 0 \tag{15}$$

thus, for stability, from the mathematical viewpoint, Δ either must be negative and $(2\sigma_\ell + \Delta(\sigma_\ell^2 + \omega_\ell^2))$ must be positive which is practically unrealistic or, practically, for positive Δ,

$$\Delta < \frac{-2\sigma_\ell}{(\sigma_\ell^2 + \omega_\ell^2)} \tag{16}$$

It can be observed that Δ will be positive as σ_ℓ is negative for a stable continuous control system. Thus the absolute maximum tolerable value of Δ is given by

$$\Delta = \min \left(\frac{-2\sigma_\ell}{\sigma_\ell^2 + \omega_\ell^2}\right) \tag{17}$$

on all ℓ where $\sigma_\ell = -\zeta_\ell \omega_\ell'$, $\omega_\ell = \sqrt{1-\zeta_\ell^2}\,\omega_\ell'$ and ω_ℓ' is the undamped natural frequency of vibration.

From the relation (17), it can be observed that the tolerable discretization step size, Δ, decreases with decreased damping ratio and increased maximum natural frequency of vibration as Δ can be approximated as $(2\zeta_\ell/\omega_\ell')$. The stability of the continuous time control system with repeated closed-loop eigenvalues is not considered here and will be attempted in the current grant period.

Example: A typical large space structure[6] with a maximum natural frequency of vibration, ω_ℓ', of 1HZ (2πrad/sec) is considered. The continuous controller is designed to provide 10% damping in all the modes and thus

$$\zeta_\ell = 0.1$$

$$\sigma_\ell = -\zeta_\ell \quad \omega'_\ell = -0.2\pi \tag{18}$$

$$\omega_\ell = \omega'_\ell \sqrt{1-\zeta_\ell^2} \cong 2\pi$$

Thus

$$\Delta < 32 \quad \text{milli-seconds} \tag{19}$$

The closed-loop control system given by

$$\dot{X} = (A + BK)X \tag{20}$$

can also be discretized as:

$$X(i+1) = e^{(A+BK)\Delta} X(i) \tag{21}$$

The eigenvalues of the matrix $e^{(A+BK)\Delta}$ are the same as the eigenvalues of the similarity matrix $T^{-1} e^{\Lambda\Delta} T$ where T and Λ are matrices given by the relations (8) and (9). As a result, the stability of the system (21) is decided by the eigenvalues of the matrix $e^{\Lambda\Delta}$. Therefore, the magnitude of the eigenvalues of the matrix $e^{\Lambda\Delta}$ must be less than 1.

i.e. $$|e^{\lambda_\ell \Delta}| < 1 \quad \text{for all } \ell \tag{22}$$

or $$|e^{(\sigma_\ell + j\omega_\ell)\Delta}| < 1 \text{ for all } \ell \tag{23}$$

And thus the following relation has to be valid for all ℓ,

$$|e^{\sigma_\ell \Delta}| < 1 \tag{24}$$

The maximum Δ can be evaluated as the minimum of the Δ_ℓ's given in relation (24). The maximum Δ given by relation (17) is an approximation of the value given by relation (23).

V.II. Computational Requirements for Estimator and Controller:

The estimator and the controller that are generally implemented using a microprocessor are described in the discrete time domain as[7]:

$$\hat{X}(i+1) = A_e \hat{X}(i) + B_e Y(i) \tag{25}$$

$$V(i) = K \hat{X}(i) \tag{26}$$

$$Y(i) = CX(i) \tag{27}$$

where

$\hat{X}$ = n x 1 estimated state vector or a transformed state vector

V = m x 1 input vector

Y = ℓx1 measurement vector

A_e, B_e, K, C are appropriately dimensioned matrices.

The minimum computational requirements are obtained through a modal transformation of the state vector, X, resulting in a diagonal system matrix A_e.

Thus the arithematic and analog to digital (A/D) conversion for sensors and digital to analog (D/A) conversion operations required to implement equations (17), (18) and (19) are as follows:

$$\begin{aligned} &\text{No. of multiplications} = n + n\ell + nm \\ &\text{No. of additions} = n\ell + nm \\ &\text{No. of A/D conversions} = \ell \\ &\text{No. of D/A conversions} = m \end{aligned} \tag{28}$$

Thus for a state of the art math-coprocessor such as Intel 80387 with 25 MHZ clock and 10 KHZ sampling rate, the following are the typical times required for various computations. (Floating point arithematic is assumed for fastness and the range of values representable.)[8]

	Clock cycles (range)	Average cycles	Instruction
Multiplication (C_m)	32-57	45	FMUL
Addition (C_a)	29-37	33	FADD
A/D conversion (A_d)	0.1 msec	-	-
D/A conversion	≃0 (negligible)	-	-

Thus assuming that the number of actuators (m) and the number of sensors (ℓ) are a fraction of the number of states (say $\ell = m = \varepsilon n$) the computational time (C_t) required to generate control signals from the continuous measurements is given by:

$$C_t = n(1+2\varepsilon n)\ C_m + n(2\varepsilon n)\ C_a + \varepsilon n\ A_d \tag{29}$$

thus

$$C_t = n(1+2\varepsilon n)\ 1.8 + 2\varepsilon n^2(1.32) + \varepsilon n(100) \text{ in } \mu \text{ seconds} \tag{30}$$

or

$$C_t = 6.24\varepsilon n^2 + n(1.8 + 100\varepsilon) \tag{31}$$

Thus the number of modes that can be handled by a microprocessor of the 80387 type to ensure stability of a large space structure with $\varepsilon = 0.25$ and $\Delta = 30$ msec can be evaluated from the equation

$$6.24\ \varepsilon n^2 + n(1.8 + 100\varepsilon) < 30x10^3 \tag{32}$$

or

$$1.56n^2 + 26.8n - 30x10^3 = 0 \tag{33}$$

thus

$$n_{1,2} = \frac{-26.8 \pm \sqrt{(26.8)^2+4x1.56x30x10^3}}{2 \text{ x } 1.56} \tag{34}$$

$$n_1 = 147.53$$

The second root of the equation (33) being negative can be neglected.

The number of modes, being equal to half the number of states, that can be handled by a microprocessor of the type 80387 is approximately equal to 74. Thus the exact discretization step size and the number of modes that can be handled by any given microprocessor can be arrived at by following the procedure given in this section and eliminating the assumptions made such as the actual times for A/D and D/A conversions, design safety factor for maximum Δ, et cetera. For a more stringent Δ value, the relation given in (24) can be used.

References

1. Kailath, T., Linear Systems, Prentice Hall, Inc., Englewood Cliffs, N.J., 1980.

2. Doyle, J., and Stein, G.,"Robustness with Observers", IEEE Trans. on AC, Vol. AC-24, No. 4, 1979, pp. 607-611.

3. Francis, B.A., A Course in H_∞ Control Theory, Springer-Verlag, New York, 1987.

4. Balas, M.J., "Discrete Time Stability of Continuous-Time Controller Designs of Large Space Structures", Journal of Guidance, Control and Dynamics, Sept.-Oct., 1982, pp. 541-543.

5. Anderson, B.D.O., and Vongpanitlerd, S., Network Analysis and Synthesis, Prentice-Hall, Inc., Englewood Cliffs, N.J., 1976, pp. 78.

6. Housner, J.M., "Structural Dynamics Model and Response of the Deployable Reference Configuration Space Station", NASA TM 86386, May 1985.

7. Farrar, F.A. and Eidens, R.S., "Microprocessor Requirements for Implementing Modern Control Logic", IEEE Trans. on AC, Vol. AC-25, June 1980, pp. 461-468.

8. Startz, R., 8087/80287/80387 for IBM PC & Compatibles, Brady, New York, 1988.

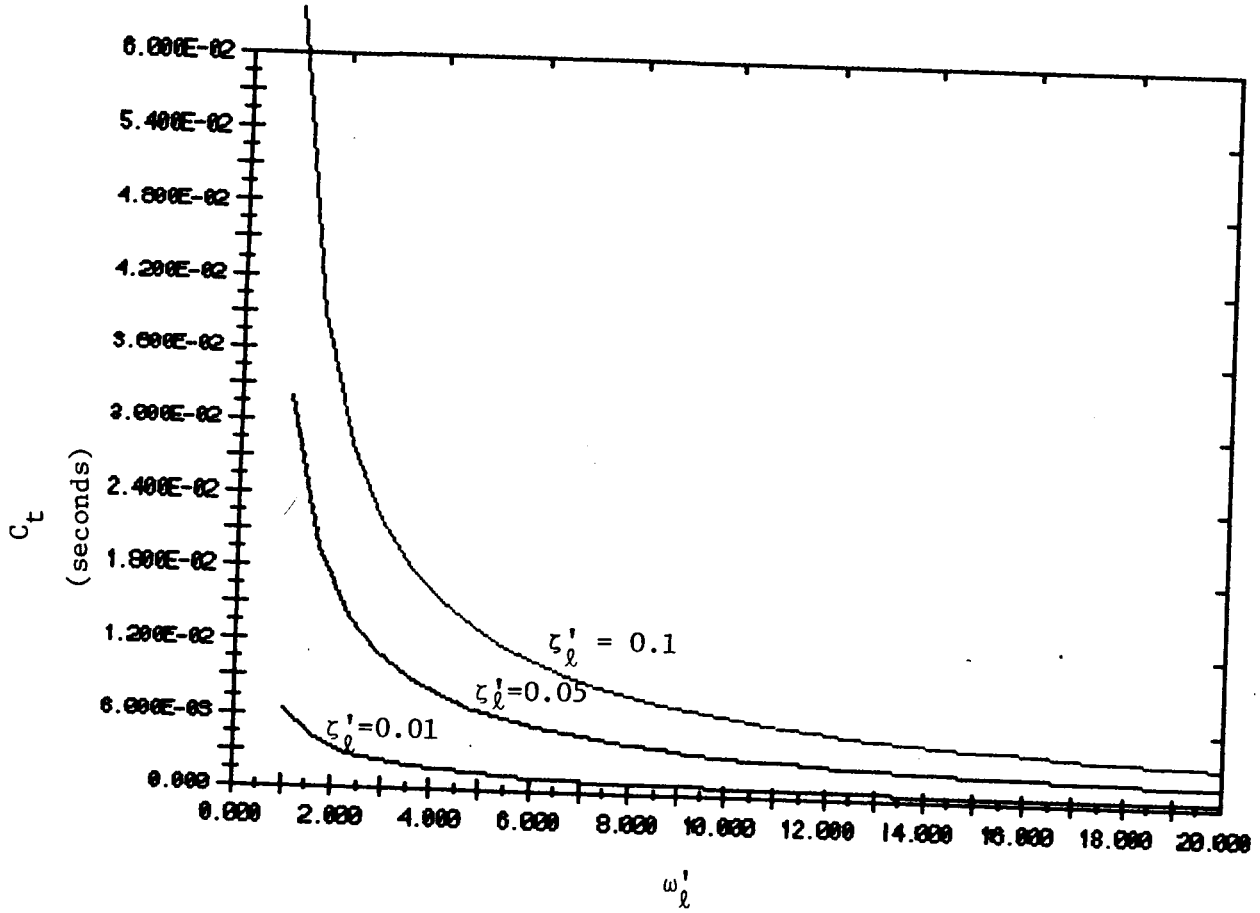

Figure v.1 Discretization Step Size vs. Undamped Natural Frequency of Vibration (ω_ℓ') as a Function of Damping ratio (ζ_ℓ')

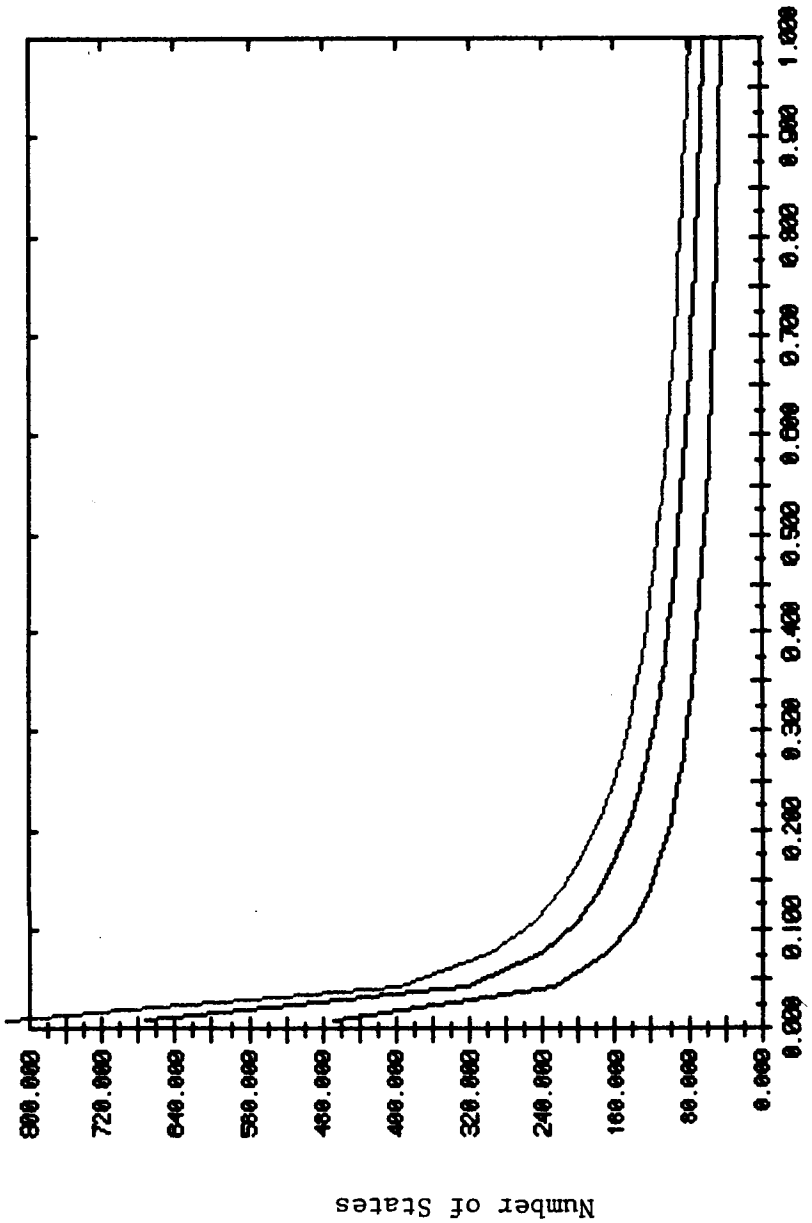

Figure v.2 Number of States vs. Number of Actuators (=sensors) as a Fraction of the Number of States (ε)

VI. CONCLUSIONS AND RECOMMENDATIONS

Mathematical models have been developed to predict the open and closed-loop dynamics of the orbiting Spacecraft Control Laboratory Experiment (SCOLE), both during station keeping and, also during rapid slewing maneuvers of up to 20 deg. amplitude. It is seen that, in the presence of gravity-gradient torques, the system assumes a new equilibrium position primarily due to the offset in the (flexible) mast attachment point to the reflector's mass center. A robust control law based on an application of the linear regulator theory can be implemented for station keeping with maximum control efforts below saturation levels.

For the slewing of a completely rigidized model of the SCOLE the LQR techniques can be extended to provide for relatively rapid slewing about each of the Shuttle's geometrical axes through amplitudes of up to 20 deg. These results can be compared with those provided by the numerical solution of the two point boundary value problem (TPBVP) associated with Pontryagin's Maximum Principle, where the slightly faster slewing times are coupled with an increase in the over-all control effort. In connection with the latter approach, the minimum time attitude slewing of a rigid spacecraft has been examined with an integral of a quadratic function of the controls used as the cost function. Both singular and nonsingular problems can be treated in a unified manner. The resulting numerical solution to the TPBVP is based on a quasilinearization algorithm. General three dimensional slewing maneuvers (e.g. SCOLE antenna line of sight slewing) can be handled.

Extensions to the important problem of minimum time and near minimum time slewing will include the effects of flexibility in the subsequent grant year. A trade-off will need to be established between the rapidity of the slewing maneuver, control effort required by the variously placed actuators, and the ability to suppress the vibrational (flexible) amplitudes during and immediately following the slew.

Finally, attention has also been focused on certain aspects of computational requirements for large space structural controller implementation. An improved stability criterion is developed for a controller, designed to function in the continuous time domain, but which receives discretized observational inputs. An expression relating the maximum tolerable discretization step size to the undamped frequency and damping ratio of any mode in the continuous time system model has been developed. Future (on board) computational requirements are evaluated based on a current state-of-the-art microprocessor , assuming that the number of actuators and sensors are a selected fraction of the number of state components. Additional future attention to computational requirements should also be based on the mathematical models of the SCOLE system whose development has been completed during this grant period.